

Thermochemical Aspects of Arene C–H Activation by Tantalum Silyl Complexes: Relative Ta–Si and Ta–C Bond Enthalpies

Qian Jiang, Doris C. Pestana, Patrick J. Carroll, and Donald H. Berry*,¹

Department of Chemistry and Laboratory for Research on the Structure of Matter, University of Pennsylvania, Philadelphia, Pennsylvania 19104-6323

Received May 2, 1994[®]

Tantalum(III) silyl complexes, $\text{Cp}_2\text{Ta}(\text{L})(\text{SiR}_3)$ ($\text{L} = \text{PMe}_3, \text{CO}$), are reactive toward the C–H bonds of unhindered arenes such as benzene, toluene, and *m*-xylene. The sterically hindered silyl complex $\text{Cp}_2\text{Ta}(\text{PMe}_3)(\text{Si}(t\text{-Bu})_2\text{H})$ (**1**) reacts in neat arenes to produce the corresponding aryl complexes, $\text{Cp}_2\text{Ta}(\text{PMe}_3)(\text{Ar})$, in high yields. However, complexes with smaller silyl ligands give equilibrium mixtures of silyl and aryl complexes in which the silyl is favored. Thermodynamic studies of this system have permitted the first direct comparison of Si–H and C–H bond activation by the same metal center and allow the estimation of relative Ta–C and Ta–Si bond dissociation enthalpies (BDE's). It is found that the Ta–Si bonds in **1** and in $\text{Cp}_2\text{Ta}(\text{PMe}_3)(\text{SiMe}_3)$ (**6**) are respectively 5.4 and 7.9 kcal mol⁻¹ weaker than the Ta–phenyl bond in $\text{Cp}_2\text{Ta}(\text{PMe}_3)(\text{Ph})$ (**3**). However, metal–phenyl bonds are generally much stronger than metal–alkyl bonds and the Ta–Si BDE's are probably comparable to or greater than the strength of a tantalum–alkyl bond. As expected, the bulkier silyl exhibits the weaker Ta–Si BDE, but surprisingly the lower stability of **1** with respect to the phenyl complex **3** is primarily due to a large and favorable entropy change (34 ± 3 eu) resulting from the release of steric congestion upon converting the silyl into the phenyl complex. The high reactivity of tantalum silyls toward arene C–H bond activation can also be combined with the facile reaction of tantalum alkyls with silanes to yield the *silane-catalyzed* conversion of $\text{Cp}_2\text{Ta}(\text{L})(\text{R})$ ($\text{R} = \text{alkyl}; \text{L} = \text{PMe}_3, \text{CH}_2=\text{CH}_2$) complexes into the corresponding aryl complexes. Complexes $\text{Cp}_2\text{Ta}(\text{PMe}_3)(\text{Si}(t\text{-Bu})_2\text{H})$ (**1**), $\text{Cp}_2\text{Ta}(\text{CO})(\text{Si}(t\text{-Bu})_2\text{H})$ (**8**), and $\text{Cp}_2\text{Ta}(\text{CO})(\text{SiMe}_3)$ (**9**) have been structurally characterized by single crystal X-ray diffraction studies.

Introduction

The activation of carbon hydrogen bonds by transition metal complexes has become one of the most studied areas of research in organometallic chemistry.² Although the ability of heterogeneous catalysts to activate arenes has been known for over 50 years,³ the direct reaction of a soluble transition metal compound with an arene to yield the aryl complex was not observed until 1965 by Chatt and Davidson.⁴ Arene C–H bond activation was reported for several additional systems in the following decade, and then in the early 1980s there were rapid advances in the number of metal complexes which react with the C–H bonds of both arenes and alkanes. Detailed mechanistic studies have led to an understanding of the factors which govern C–H bond activation, and elucidation of several distinct mechanisms by which C–H bonds are cleaved. Recently, greater attention has been paid to the thermodynamics of C–H activation, and in particular there has been an increased effort to determine the metal–hydrogen and metal–carbon bond dissociation enthal-

pies (BDE's) which are so closely linked to the viability of this and other important reactions.⁵ The bonding energetics of elements other than carbon to transition metals have also been examined, although these studies have been almost entirely limited to elements in the same period as carbon.⁶

The last several years have also witnessed a renaissance in the chemistry of metal–silicon compounds, with the synthesis of many new structural types^{7–12} and the development of new stoichiometric and catalytic reactions involving organosilanes.^{13,14} However, the

(5) For recent reviews, see: (a) *Bonding Energetics in Organometallic Compounds*; Marks, T. J., Ed.; ACS Symposium Series 428; American Chemical Society: Washington, DC, 1990. (b) Martinho Simões, J. A.; Beauchamp, J. M. *Chem. Rev.* **1990**, *90*, 629.

(6) Bryndza, H. E.; Domaille, P. J.; Tam, W.; Fong, L. K.; Paciello, R. A.; Bercaw, J. E. *Polyhedron* **1988**, *7*, 1441.

(7) (a) Tilley, T. D. In *The Chemistry of Organic Silicon Compounds*; Patai, S., Rappoport, Z., Eds.; Wiley: New York, 1989; Vol. 2. (b) Tilley, T. D. In *The Silicon-Heteroatom Bond*; Patai, S., Rappoport, Z., Eds.; Wiley: New York, 1991; Chapters 9 and 10.

(8) (a) Campion, B. K.; Heyn, R.; Tilley, T. D. *J. Am. Chem. Soc.* **1988**, *110*, 7558. (b) Campion, B. K.; Heyn, R.; Tilley, T. D. *J. Am. Chem. Soc.* **1990**, *112*, 4079. (c) Campion, B. K.; Heyn, R.; Tilley, T. D. *J. Am. Chem. Soc.* **1993**, *115*, 5527. (d) Koloski, T. S.; Carroll, P. J.; Berry, D. H. *J. Am. Chem. Soc.* **1990**, *112*, 6405. (e) Koloski, T. S. Ph.D. Dissertation, University of Pennsylvania, 1991. (f) Koloski, T. S.; Carroll, P. J.; Berry, D. H. Manuscript in preparation. (g) Ando, W.; Yamamoto, T.; Saso, H.; Kabe, Y. *J. Am. Chem. Soc.* **1991**, *113*, 2791.

(9) (a) Berry, D. H.; Chey, J. C.; Zipin, H. S.; Carroll, P. J. *J. Am. Chem. Soc.* **1990**, *112*, 452. (b) Berry, D. H.; Chey, J. C.; Zipin, H. S.; Carroll, P. J. *Polyhedron* **1991**, *10*, 1189. (c) Pham, E. K.; West, R. J. *Am. Chem. Soc.* **1989**, *111*, 7667. (d) Pham, E. K.; West, R. *Organometallics* **1990**, *9*, 1517.

[®] Abstract published in *Advance ACS Abstracts*, August 1, 1994.

(1) Alfred P. Sloan Research Fellow, 1990–1994.

(2) For reviews, see: (a) Green, M. L. H.; O'Hare, D. *Pure Appl. Chem.* **1985**, *57*, 1897. (b) Crabtree, R. H. *Chem. Rev.* **1985**, *85*, 245. (c) Deem, M. L. *Coord. Chem. Rev.* **1986**, *74*, 101. (d) Bergman, R. G. *Science* **1984**, *223*, 902. (e) Jones, W. D.; Feher, F. J. *Acc. Chem. Res.* **1989**, *22*, 91.

(3) Farkas, A.; Farkas, L. *Trans. Faraday Soc.* **1937**, *33*, 827.

(4) Chatt, J.; Davidson, J. M. *J. Chem. Soc.* **1965**, 843–855.

thermochemical properties of the metal–silicon bond have been largely ignored, with the notable exception of a recent study by Marks and co-workers in which a uranium–silicon bond dissociation energy (BDE) was determined by calorimetric methods.¹⁵ Given the current paucity of thermochemical data, it is difficult to address even the most basic questions regarding the strength of metal–silicon bonds in any general sense.

The present contribution describes the reversible oxidative addition of arene C–H bonds to tantalum silyl complexes under extremely mild thermal conditions and a study of the thermochemical stability of tantalum silyl and phenyl complexes from which relative Ta–C and Ta–Si bond strengths have been determined. In addition, entropy, and not enthalpy, has been found to exert the predominant role in destabilizing a sterically hindered silyl complex. Some of this work has been published previously in preliminary form.¹⁶

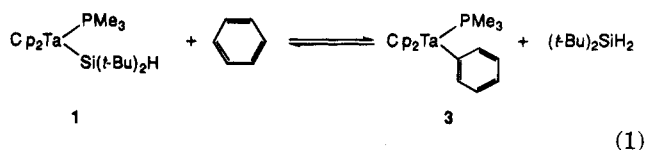
Results and Discussion

I. Reaction of $\text{Cp}_2\text{Ta}(\text{PMe}_3)(\text{SiR}_3)$ with Arenes.

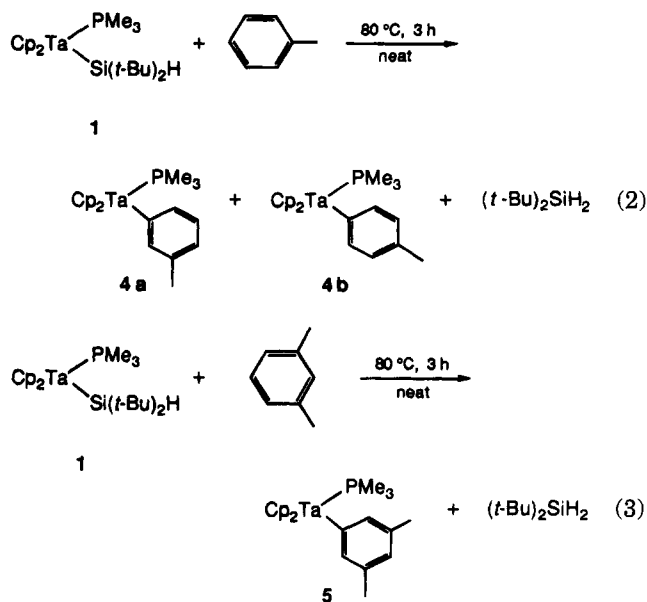
We recently reported a general synthetic route to tantalum(III) silyl complexes, $\text{Cp}_2\text{Ta}(\text{PMe}_3)(\text{SiR}_3)$, and described the preparation and characterization of several members of the series. In particular, the di-*tert*-butylsilyl complex $\text{Cp}_2\text{Ta}(\text{PMe}_3)(\text{Si}(t\text{-Bu})_2\text{H})$ (**1**), prepared from $\text{Cp}_2\text{Ta}(\text{PMe}_3)(\text{CH}_3)$ (**2**) and di-*tert*-butylsilane, exhibits an unusually labile PMe_3 ligand as a result of the steric bulk of the silyl group and shows unique reactivity in a variety of processes under very mild

conditions, including the activation of C–H¹⁷ and B–H¹⁸ bonds and alkylidene transfer reactions.¹⁹

Compound **1** readily reacts with stoichiometric amounts of benzene in nonaromatic solvents to yield equilibrium mixtures that contain the phenyl complex, $\text{Cp}_2\text{Ta}(\text{PMe}_3)(\text{Ph})$ (**3**), and di-*tert*-butylsilane. In pure benzene, however, this equilibrium is shifted almost entirely to the right and reaches completion within 5 days at 25 °C, or 2 h at 70 °C, and thus affords a preparative route to the tantalum phenyl complex **3**, as reported previously¹⁶ and shown in eq 1.



Similarly, **1** reacts with toluene and *m*-xylene to yield the corresponding tolyl and xylyl complexes and di-*tert*-butylsilane. Although there are four different types of C–H bonds in toluene, only those on the meta and para positions are reactive. Selectively decoupled ¹H NMR spectra of the products show that only *m*- (**4a**) and *p*-tolyl (**4b**) complexes are formed in a ca. 2:1 ratio (eq 2), reflecting a statistical distribution for the reaction of



1 toward the *meta* and *para* positions of toluene. The *o*-tolyl and benzyl complexes were not detected by NMR.¹⁹ In the case of the reaction with *m*-xylene, only the *m*-xylyl complex **5** is formed (eq 3). In contrast, compound **1** is virtually inert toward both *p*-xylene and mesitylene, substrates which only have *o*-C–H bonds, presumably due to adverse steric interactions. Thermolysis of **1** in these arene solvents leads to decomposition and formation of several unidentified products. Spectroscopic data for **4a**, **4b**, and **5** are listed in Table 1.

Complexes of less bulky silyl ligands exhibit decreased reactivity toward benzene. Thermolysis of the tri-

(17) Jiang, Q.; Carroll, P. J.; Berry, D. H. *Organometallics* **1991**, *10*, 3648.

(18) Jiang, Q.; Carroll, P. J.; Berry, D. H. *Organometallics* **1993**, *12*, 177.

(19) Berry, D. H.; Koloski, T. S.; Carroll, P. J. *Organometallics* **1990**, *9*, 2952.

(10) (a) Straus, D. A.; Tilley, T. D.; Rheinhold, A. L.; Geib, S. J. *J. Am. Chem. Soc.* **1987**, *109*, 5872. (b) Straus, D. A.; Zhang, C.; Quimbata, G. E.; Grumbine, S. D.; Heyn, R. H.; Tilley, T. D.; Rheinhold, A. L.; Geib, S. J. *J. Am. Chem. Soc.* **1990**, *112*, 2673. (c) Grumbine, S. D.; Chadha, R. K.; Tilley, T. D. *J. Am. Chem. Soc.* **1992**, *114*, 1518. (d) Leis, C.; Zybilla, C.; Lachmann, J.; Müller, G. *Polyhedron* **1991**, *11*, 1163. (e) Zybilla, C. *Top. Curr. Chem.* **1991**, *160*, 1. (f) Probst, R.; Leis, C.; Gamper, E.; Herdtweck, E.; Zybilla, C. *Angew. Chem., Int. Ed. Engl.* **1991**, *30*, 1132. (g) Leis, C.; Wilkinson, D.; Handwerker, H.; Zybilla, C.; Müller, G. *Organometallics* **1992**, *11*, 514. (h) Ueno, K.; Tobita, H.; Shimoi, M.; Ogino, H. *J. Am. Chem. Soc.* **1988**, *110*, 4092. (i) Tobita, H.; Ueno, K.; Shimoi, M.; Ogino, H. *J. Am. Chem. Soc.* **1990**, *112*, 3415. (j) Takeuchi, T.; Tobita, H.; Ogino, H. *Organometallics* **1991**, *10*, 835.

(11) (a) Straus, D. A.; Grumbine, S. D.; Tilley, T. D. *J. Am. Chem. Soc.* **1990**, *112*, 7801. (b) Grumbine, S. D.; Tilley, T. D.; Rheinhold, A. L. *J. Am. Chem. Soc.* **1993**, *115*, 358. (c) Grumbine, S. D.; Tilley, T. D.; Rheinhold, A. L.; Arnold, F. P. *J. Am. Chem. Soc.* **1993**, *115*, 7884.

(12) (a) Procopio, L. J.; Carroll, P. J.; Berry, D. H. *J. Am. Chem. Soc.* **1991**, *113*, 1870. (b) Procopio, L. J.; Carroll, P. J.; Berry, D. H. *Organometallics* **1993**, *12*, 3087.

(13) For examples of new catalytic Si–Si bond forming reactions, see: (a) Aitken, C. T.; Harrod, J. F.; Samuel, E. *J. Am. Chem. Soc.* **1986**, *108*, 4059. (b) Tilley, T. D. *Acc. Chem. Res.* **1993**, *26*, 22 and references therein. (c) Nakano, T.; Nakamura, H.; Nagai, Y. *Chem. Lett.* **1989**, 83. (d) Hengge, E.; Weinberger, M.; Jammegg, C. *J. Organomet. Chem.* **1991**, *410*, C1. (e) Corey, J. Y.; Zhu, X.-H.; Bedard, T. C.; Lange, L. D. *Organometallics* **1991**, *10*, 924. (f) Yamashita, H.; Tanaka, M.; Goto, M. *Organometallics* **1992**, *11*, 3227.

(14) For examples of new catalytic Si–C, Si–N, and Si–O bond forming reactions, see: (a) Procopio, L. J.; Berry, D. H. *J. Am. Chem. Soc.* **1991**, *113*, 4039. (b) Procopio, L. J.; Mayer, B.; Plössl, K.; Berry, D. H. *Polym. Prepr. (Am. Chem. Soc., Div. Polym. Chem.)* **1992**, *33*, 1241. (c) Laine, R. M.; Blum, Y. D.; Tse, D.; Glaser, R. In *Inorganic and Organometallic Polymers*; Zeldin, M.; Wynne, K. J., Allcock, H. R., Eds.; ACS Symposium Series 360; American Chemical Society: Washington, DC, 1988. (d) Luo, X. L.; Crabtree, R. H. *J. Am. Chem. Soc.* **1989**, *111*, 2527. (e) Uchimarui, Y.; El-Sayed, A. M. M.; Tanaka, M. *Organometallics* **1993**, *12*, 2065. (f) Ishikawa, M.; Okazaki, S.; Naka, A.; Sakamoto, H. *Organometallics* **1992**, *11*, 4135. (g) Ishikawa, M.; Sakamoto, H.; Okazaki, S.; Naka, A. *J. Organomet. Chem.* **1992**, *439*, 19.

(15) Nolan, S. P.; Porchia, M.; Marks, T. J. *Organometallics* **1991**, *10*, 1450.

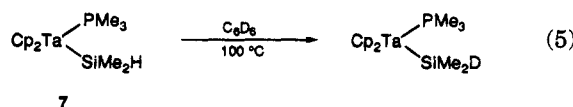
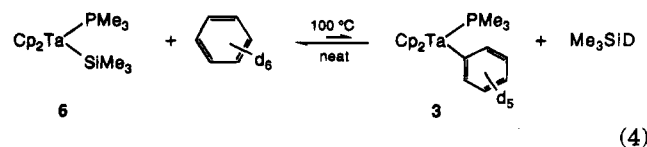
(16) Berry, D. H.; Jiang, Q. *J. Am. Chem. Soc.* **1989**, *111*, 8049.

Table 1. NMR Data

compd	¹ H NMR ^a	¹³ C{ ¹ H} NMR	³¹ P{ ¹ H} NMR ^b
4a	7.58 (s, 1H, 2-C ₆ H ₄)	158.1 (d, J _{PC} = 5, <i>ipso</i> -C ₆ H ₄)	-24.8
	7.49 (d, J = 7.3, 1H, 6-C ₆ H ₄)	148.5 (d, J _{PC} = 4, <i>o</i> -C ₆ H ₄)	
	6.99 (t, J = 7.3, 1H, 5-C ₆ H ₄)	145.7 (d, J _{PC} = 5, <i>o</i> -C ₆ H ₄)	
	6.86 (d, J = 7.3, 1H, 4-C ₆ H ₄)	133.0 (s, 3-C ₆ H ₄)	
	4.37 (d, J = 1.9, 10H, C ₅ H ₅)	125.2 (s, 5-C ₆ H ₄)	
	2.33 (s, 3H, 3-CH ₃)	121.9 (s, <i>p</i> -C ₆ H ₄)	
	0.97 (d, J = 7.2, 9H, PCH ₃)	86.5 (s, C ₅ H ₅)	
		22.1 (s, 3-CH ₃)	
4b	7.59 (d, J = 7.5, 2H, <i>o</i> -C ₆ H ₄)	(<i>ipso</i> -C ₆ H ₄) ^c	-24.8
	6.91 (d, J = 7.5, 2H, <i>m</i> -C ₆ H ₄)	149.4 (d, J _{PC} = 4, <i>o</i> -C ₆ H ₄)	
	4.36 (d, J = 2.0, 10H, C ₅ H ₅)	129.4 (s, <i>p</i> -C ₆ H ₄)	
	2.35 (s, 3H, <i>p</i> -CH ₃)	126.7 (s, <i>m</i> -C ₆ H ₄)	
	0.96 (d, J = 7.2, 9H, PCH ₃)	86.4 (s, C ₅ H ₅)	
		21.0 (d, J _{PC} = 24, PCH ₃)	
5	7.38 (s, 2H, <i>o</i> -C ₆ H ₅)	157.6 (d, J _{PC} = 5, <i>ipso</i> -C ₆ H ₅)	-24.9
	6.63 (s, 1H, <i>p</i> -C ₆ H ₅)	146.7 (d, J _{PC} = 5, <i>o</i> -C ₆ H ₅)	
	4.39 (d, J = 1.9, 10H, C ₅ H ₅)	132.8 (s, <i>m</i> -C ₆ H ₅)	
	2.33 (s, 6H, <i>m</i> -CH ₃)	123.1 (s, <i>p</i> -C ₆ H ₅)	
	1.00 (d, J = 7.1, 9H, PCH ₃)	86.4 (s, C ₅ H ₅)	
		21.9 (s, <i>m</i> -CH ₃)	
		21.0 (d, J _{PC} = 25, PCH ₃)	
11	8.00 (d, J = 7.8, 2H, <i>o</i> -C ₆ H ₅)	152.5 (s, <i>ipso</i> -C ₆ H ₅)	
	7.35 (t, J = 7.8, 2H, <i>m</i> -C ₆ H ₅)	144.7 (d, J _{CH} = 153, <i>o</i> -C ₆ H ₅) ^d	
	7.22 (t, J = 7.8, 1H, <i>p</i> -C ₆ H ₅)	127.1 (d, J _{CH} = 154, <i>m</i> -C ₆ H ₅)	
	4.47 (s, 10H, C ₅ H ₅)	122.7 (d, J _{CH} = 158, <i>p</i> -C ₆ H ₅)	
	1.05 (s, 4H, C ₂ H ₄)	97.5 (d, J _{CH} = 178, C ₅ H ₅)	
		23.6 (t, J _{CH} = 152, C ₂ H ₄)	
	17.8 (t, J _{CH} = 151, C ₂ H ₄)		

^a Chemical shifts are in ppm upfield from TMS. Coupling constants are in Hz. ^b Chemical shifts are in ppm upfield from 85% H₃PO₄. ^c Not observed. ^d J_{CH} values were obtained from ¹H coupled spectra.

methylsilyl complex, Cp₂Ta(PMe₃)(SiMe₃) (**6**), in benzene-*d*₆ at 100 °C for 2 h results in an equilibrium mixture containing only 2% **3** and Me₃SiD (eq 4). In the case of



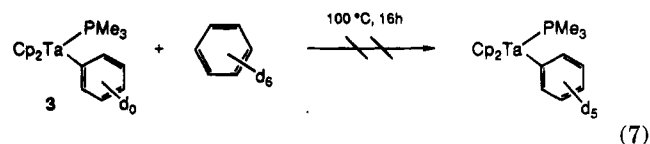
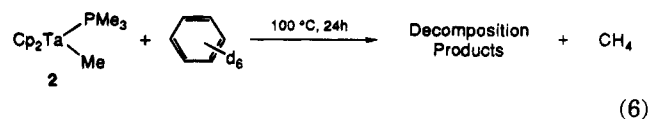
Cp₂Ta(PMe₃)(SiMe₂H) (**7**), compound **3** cannot be detected by ¹H NMR, although deuteration of Si-H is observed, apparently by exchange with benzene-*d*₆ (eq 5).

An apparent key to the greater rate of C-H activation by **1** versus **6** is the lability of the phosphine ligand. For example, **1** reacts rapidly with carbon monoxide at room temperature to yield the carbonyl derivative Cp₂Ta(CO)(Si(*t*-Bu)₂H) (**8**),¹⁷ whereas **6** exchanges CO for PMe₃ to form Cp₂Ta(CO)(SiMe₃) (**9**) only after hours at >100 °C. Furthermore, the more labile PMe₃ in **1** can be trapped as the borane adduct as it dissociates at 25 °C, but **6** is inert at temperatures below ca. 100 °C.¹⁸ It is not surprising, therefore, that the activation of arenes by **1** is inhibited by added free PMe₃. For example, **1** reacts with neat benzene ca. 4 times slower in the presence of 3 equiv of PMe₃, consistent with initial phosphine dissociation prior to the C-H activation step.

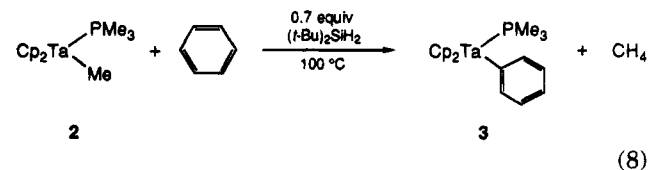
Carbonyl adduct **8** also reacts with neat benzene to form Cp₂Ta(CO)(Ph) (**10**), but the reaction is slower than

in the case of **1** (days at >90 °C), and only proceeds to ca. 20% conversion to the phenyl complex at equilibrium. The lower rate of C-H activation is consistent with the relatively low lability of the carbonyl ligand, whereas the change in the relative thermodynamics of the silyl and the phenyl complexes is more easily understood in light of the structural and dynamic NMR studies that will be described in section III.

In contrast to the silyl complexes, tantalum alkyl or aryl complexes are virtually inert toward arene solvents under the same conditions. Thermolysis of Cp₂Ta(PMe₃)(Me) (**2**) in benzene-*d*₆ at 100 °C for 24 h leads to decomposition of the methyl complex to a complicated mixture of products. A small Cp signal (3% of the total tantalum compounds) in the ¹H NMR spectrum appears at the correct chemical shift for the phenyl complex **3**, but the observation of CH₄, rather than CH₃D, suggests it does not arise from the direct reaction of **2** with benzene-*d*₆ (eq 6). Similarly, thermolysis of Cp₂Ta(PMe₃)(Ph) (**3**) in benzene-*d*₆ results in no observable deuteration of the phenyl group, but only decomposition after 16 h at 100 °C (eq 7).

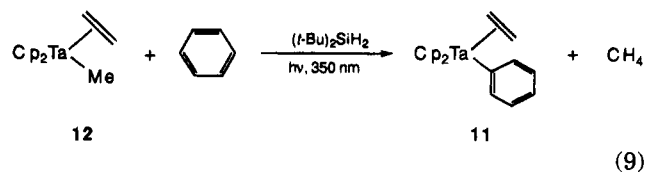


Although the methyl complex **2** does not react directly with aryl C-H bonds, reactions with the silane Si-H bonds are very facile and form the basis of a general synthetic route to tantalocene silyls.¹⁷ This fact, combined with the reactivity of the silyls toward arenes, suggested it might be possible to catalyze the reaction of **2** with arenes using silanes. Indeed, **2** reacts with benzene in the presence of 0.7 equiv of di-*tert*-butylsilane quantitatively to yield **3** and CH₄ within 4 h at 100 °C (eq 8). That this reaction can be achieved catalytically

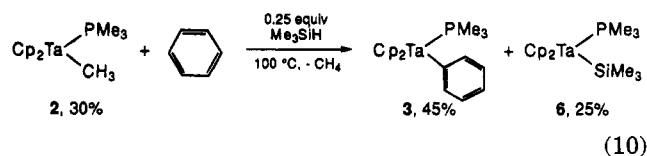


clearly indicates there is no thermodynamic obstacle to the methyl to phenyl complex conversion and points to a kinetic barrier for arene C-H activation by the alkyl. In any case, the silane-catalyzed reaction offers a convenient synthetic route to the aryl complexes directly from **2**. In this manner, compound **3** has been isolated in 91% yield. Similarly, the ethylene phenyl complex Cp₂Ta(CH₂=CH₂)(Ph) (**11**) has been prepared by the photolysis of Cp₂Ta(CH₂=CH₂)(CH₃) (**12**) with benzene in the presence of di-*tert*-butylsilane (eq 9).

Smaller silanes also promote the activation of C-H bonds by **2**. In the presence of 0.25 equiv of Me₃SiH, thermolysis of **2** at 100 °C in benzene for 2 h produces **3** in 45% yield (by ¹H NMR), along with Cp₂Ta(PMe₃)(SiMe₃) (**6**) (25%) and unreacted starting material (30%)



(eq 10). Higher conversions can be achieved with longer reaction times, but are accompanied by decomposition.



II. Molecular Structures of $\text{Cp}_2\text{Ta(L)(SiR}_3)$ **1, **8**, and **9**.** Steric factors clearly play a role in determining the greater reactivity of **1** relative to **6**, thus structural studies were undertaken to more precisely examine the effect of the different silyl groups on the ground state geometry of the complexes. The molecular structures of di-*tert*-butylsilyl complexes **1** and **8** and trimethylsilyl carbonyl complex **9**, as determined by single crystal X-ray diffraction studies, are shown in Figures 1–3. Crystallographic details and selected bond distances and angles are listed in Tables 2–4. In addition, the structure of $\text{Cp}_2\text{Ta(PMe}_3)(\text{SiMe}_3)$ (**6**) was recently described¹⁷ and will be included in the present discussion.

Complexes **1**, **6**, **8**, and **9** exhibit similar molecular geometries, with the tantalum atoms in pseudotetrahedral environments consisting of two Cp centroids, the ligand L (CO or PMe_3), and the silicon atom. Other structural parameters vary according to the electronic and steric factors of ligands L and the silyl groups. Interestingly, the Cp–Ta–Cp angles in these complexes appear to be essentially unaffected by the size of the silyl groups, but are rather more sensitive to the nature of L. Despite the large difference in the silyls, the angles in the two carbonyl complexes (141.7° in **8** and 141.8° in **9**) are nearly identical and significantly larger than those found in the two PMe_3 complexes (135.6° in **1** and 134.9° in **6**). This order is opposite to that predicted by Lauer and Hoffmann, who suggested that better σ -electron donating ligands would lead to an increase in the Cp–M–Cp angle.²⁰ The effect of ancillary ligands on metal–silicon bond lengths in *trans*-(CO)₄Mn(SiMe₃)(L) has been examined by Couldwell and Simpson,²¹ who found that replacement of CO with the better σ -donor but poorer π -acceptor PPh_3 results in a shortening of the M–Si bond. This was interpreted as the result of an overall increase in electron density at manganese, particularly in orbitals of π -symmetry which could be used in π -back-bonding to strengthen the Mn–Si bond. However, electron density does not appear to play a comparable role in the present tantalum complexes. Rather, the Ta–Si bond distances seem most sensitive to the size of the silyls. Complexes $\text{Cp}_2\text{Ta(PMe}_3)(\text{SiMe}_3)$ (**6**) and $\text{Cp}_2\text{Ta(CO)(SiMe}_3)$ (**9**) exhibit similar Ta–Si bond lengths ($2.639(4)$ and $2.631(2)$ Å),

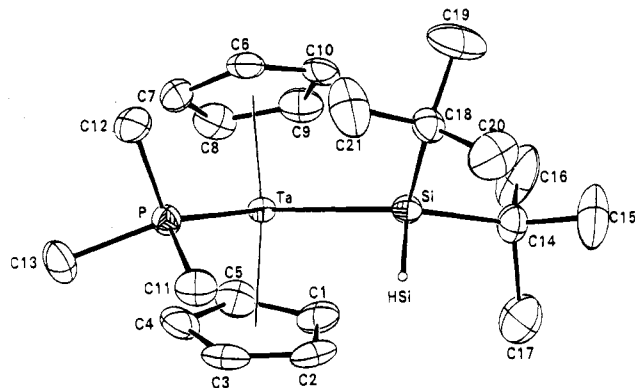


Figure 1. ORTEP drawing of $\text{Cp}_2\text{Ta(PMe}_3)(\text{Si}(t\text{-Bu})_2\text{H})$, **1**, showing 30% probability thermal ellipsoids.

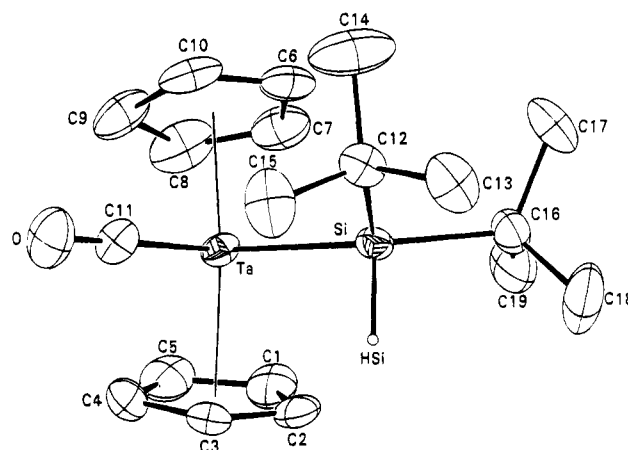


Figure 2. ORTEP drawing of $\text{Cp}_2\text{Ta(CO)(Si}(t\text{-Bu})_2\text{H})$, **8**, showing 30% probability thermal ellipsoids.

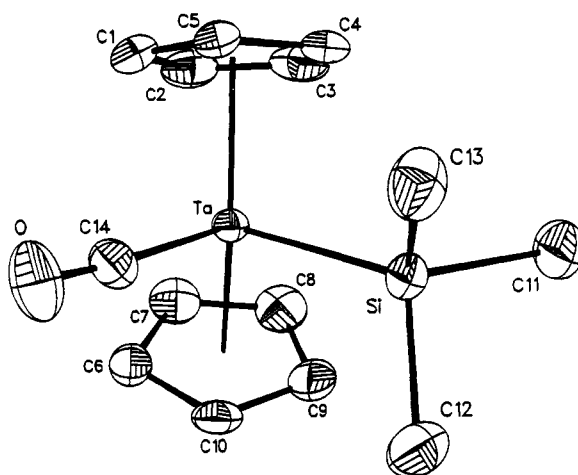


Figure 3. ORTEP drawing of $\text{Cp}_2\text{Ta(CO)(SiMe}_3)$, **9**, showing 30% probability thermal ellipsoids.

which are comparable to previously reported values.^{17,22} Replacement of trimethylsilyl with sterically bulky di-*tert*-butylsilyl, however, leads to a remarkable increase in the Ta–Si bond length, and $\text{Cp}_2\text{Ta(CO)(Si}(t\text{-Bu})_2\text{H})$ (**8**) exhibits a Ta–Si bond distance of $2.684(1)$ Å, 0.053 Å longer than the bond in **9**. Furthermore, the Ta–Si bond distance increases by over 0.1 Å in going from $\text{Cp}_2\text{Ta(PMe}_3)(\text{SiMe}_3)$ ($2.639(4)$ Å) to $\text{Cp}_2\text{Ta(PMe}_3)(\text{Si}(t\text{-Bu})_2\text{H})$ ($2.749(4)$ Å).

(20) Lauer, J.; Hoffman, R. *J. Am. Chem. Soc.* **1976**, *98*, 1729.

(21) Couldwell, M. C.; Simpson, J. *J. Chem. Soc., Dalton Trans.* **1976**, 714.

(22) (a) Arnold, J.; Tilley, T. D. *Organometallics* **1987**, *6*, 473. (b) Arnold, J.; Shina, D. W.; Tilley, T. D. *Organometallics* **1986**, *5*, 2037. (c) Curtis, M. D.; Bell, L. G.; Butler, W. M. *Organometallics* **1985**, *4*, 701.

Table 2. Summary of Structure Determination^a of Compounds 1, 8, and 9

	1	8	9
formula	TaC ₂₁ H ₃₈ PSi	TaC ₁₉ H ₂₉ SiO	TaC ₁₄ H ₁₉ SiO
fw	530.55	482.48	412.34
cryst dimens (mm)	0.55 × 0.45 × 0.30	0.70 × 0.35 × 0.26	0.55 × 0.50 × 0.23
cryst class	orthorhombic	monoclinic	orthorhombic
space group	P2 ₁ 2 ₁ 2 ₁ (No. 19)	C2/c (No. 15)	P2 ₁ 2 ₁ 2 ₁ (No. 19)
Z	4	8	4
cell constants			
<i>a</i> (Å)	13.593(2)	26.163(4)	7.464(2)
<i>b</i> (Å)	10.216(1)	8.800(1)	13.280(2)
<i>c</i> (Å)	16.007(3)	17.397(3)	14.857(5)
β (deg)		107.08(1)	
<i>V</i> (Å ³)	2223(1)	3829(2)	1473(1)
μ (cm ⁻¹)	50.13	57.37	74.42
trans (%) (min, max, av) ^b	64.72, 99.79, 84.20	52.83, 99.86, 81.78	36.30, 99.97, 65.56
<i>D</i> _{calc} (g cm ⁻³)	1.585	1.674	1.860
<i>F</i> (000)	1064	1904	792
<i>h, k, l</i> collected	+17, +13, ±20	±33, +11, +22	+9, +17, +19
no. of reflns measd	5601	4818	1970
no. of unique reflns	5075	4387	1948
no. of reflns used in refinement (<i>F</i> ² > 3.0σ)	4632	3424	1829
no. of params	217	199	154
data/param ratio	21.3	17.2	11.9
<i>R</i> ₁	0.025	0.025	0.026
<i>R</i> ₂	0.034	0.033	0.036
GOF	1.125	1.144	1.474

^a Radiation: Mo Kα ($\lambda = 0.71073 \text{ \AA}$); θ range = 2.0–27.5°; scan mode ω -2 θ . ^b Absorption correction (Ψ scans) when applied.

Table 3. Selected Bond Distances (Å) in Complexes 1, 8, and 9^a

compd	Ta–Si	Ta–L ^b	Si–C	L ^a
1	2.740(1)	Ta–P, 2.543(1)	Si–C14, 1.975(6) Si–C18, 1.985(6)	P–C11, 1.835(7) P–C12, 1.821(6) P–C13, 1.823(7)
8	2.684(1)	Ta–C11, 2.009(5)	Si–C12, 1.947(5) Si–C16, 1.970(5)	O–C11, 1.165(6)
9	2.631(2)	Ta–C14, 2.044(7)	Si–C11, 1.93(1) Si–C12, 1.901(9) Si–C13, 1.924(9)	O–C14, 1.135(9)

^a Numbers in parentheses are estimated standard deviations in the least significant digits. ^b L = CO or PMe₃.

Bu)₂H) (2.740(1) Å). It is also noteworthy that the Ta–Si bond lengths in the two di-*tert*-butylsilyl complexes are quite different and that the more electron rich phosphine complex exhibits the longer Ta–Si bond. The extremely long bond distance in **1** can be attributed to the combined steric hindrance of di-*tert*-butylsilyl and PMe₃ groups in **1**, which destabilizes the molecule and leads to the high reactivity of this complex as described above. Although **8** also contains the bulky silyl ligand, the smaller size of the carbonyl ancillary ligand apparently permits a somewhat closer approach of the Ta and Si centers. As a final point regarding these structures, it should be noted that the di-*tert*-butylsilyl ligands in **1** and **8** are oriented in the equatorial wedge so as to minimize interactions of the *tert*-butyl groups with the Cp rings. The net result is that one *tert*-butyl group points to the outside of the wedge and the other points toward the carbonyl or phosphine ligand and slightly toward one Cp. It is this inequivalence of the *tert*-butyl and Cp groups which forms the basis of the dynamic NMR studies described in the next section.

III. Solution NMR Studies of the Dynamic Behavior of Di-*tert*-butylsilyl Complexes 1 and 8. The steric congestion in the bulky silyl complexes **1** and **8** has also been probed with variable temperature ¹H NMR studies. The ¹H NMR spectrum of **1** at 298 K consists of four resonances: two sharp singlets for the

SiH and *tert*-butyl groups, and two sharp doublets for the Cp and phosphine ligands. The Cp peak decoalesces as the temperature is decreased, and two resonances (δ 4.24 and 4.10) are observed at 213 K. Coupling of the Cp H's to phosphorus is observed in the 298–263 K interval (³J_{P–H} = 2.5 Hz), but this information is lost as the signal broadens and decoalesces at lower temperatures. The process is completely reversible. Coalescence is observed at 226 K ($\Delta G^\ddagger = 10.9 \text{ kcal mol}^{-1}$). The *tert*-butyl resonance also broadens as the temperature is decreased, but decoalescence is not observed at the lowest temperature obtained (213 K). In contrast, the coalescence temperature (*T*_c) for the Cp resonance in **8** is 313 K ($\Delta G^\ddagger = 15.4 \text{ kcal mol}^{-1}$), nearly 90 °C above that observed for **1**. The ¹H NMR spectrum of **8** at 298 K exhibits two broad peaks each for the Cp and the *tert*-butyl groups. Both pairs of broad signals coalesce gradually as the temperature is increased. The coalescence of the *tert*-butyl resonance is observed at 320 K, slightly higher than that for the Cp resonances. Interconversion of the inequivalent Cp ligands arises from rotation of the di-*tert*-butylsilyl group; thus the ΔG^\ddagger values obtained from coalescence temperatures represent the barrier to rotation around the Ta–Si bond.

As described in section I, the two di-*tert*-butylsilyl complexes, Cp₂Ta(PMe₃)(Si(*t*-Bu)₂H) (**1**) and Cp₂Ta(CO)(Si(*t*-Bu)₂H) (**8**), react quite differently, with the phosphine derivative being more reactive in all cases. Furthermore, the structural studies described above reveal a Ta–Si bond in **1** which is substantially longer than that in **8** or **6**. It appears, therefore, that the combination of bulky silyl and PMe₃ ligands in **1** yields the most sterically destabilized complex of the series. The bulky silyl carbonyl **8** is somewhat less destabilized than **1**, and the SiMe₃ complexes are the least hindered. Indeed, it is not surprising that **1** and **8** exhibit variable temperature ¹H NMR spectra which indicate hindered rotation at the Ta–Si bond. It was not initially expected, however, that the most sterically encumbered

Table 4. Selected Bond Angles (deg) in Compounds 1, 8, and 9^a

compd	Cp1-Ta-Cp2 ^b	Si-Ta-L ^c	Ta-Si-C	C-Si-C	Ta-L ^c
1	135.6	Si-Ta-P, 93.8(1)	Ta-Si-C14, 115.9(2) Ta-Si-C18, 122.4(2)	C14-Si-C18, 107.3(3)	Ta-P-C11, 120.1(2) Ta-P-C12, 119.4(2) Ta-P-C13, 116.2(2)
8	141.7	Si-Ta-C11, 92.8(2)	Ta-Si-C12, 119.5(2) Ta-Si-C16, 117.5(2)	C12-Si-C16, 110.6(2)	Ta-C11-O, 173.5(5)
9	141.8	Si-Ta-C14, 86.7(2)	Ta-Si-C11, 115.7(3) Ta-Si-C12, 115.4(3) Ta-Si-C13, 114.3(3)	C11-Si-C12, 102.4(4) C11-Si-C13, 105.4(4) C12-Si-C13, 102.0(4)	Ta-C14-O, 175.9(8)

^a Numbers in parentheses are estimated standard deviations in the least significant digits. ^b Cp1 and Cp2 refer to the C₅H₅ centroids. ^c L = PMe₃ and CO.

complex, **1**, would exhibit a barrier to rotation which is 4.5 kcal mol⁻¹ lower than that for the apparently less crowded **8**.

This apparent discrepancy can be resolved by separating the issue of the total steric hindrance in the complexes, as indicated by thermodynamic stability and ligand lability in the ground state structure, from the specific issue of the barrier to rotation around the Ta-Si bond. Note that the barrier to Ta-Si bond rotation is determined by the difference between the energy of the ground state geometry and the higher energy symmetrical transition state in which both *tert*-butyl groups are thrust directly into the Cp rings. The carbonyl ligand in **8** is smaller than the phosphine in **1**; therefore the silyl ligand is able to approach the tantalum center in the ground state geometry of **8** more closely than in **1** and thus **8** exhibits the shorter Ta-Si bond. However, bringing the di-*tert*-butylsilyl group closer to the metal destabilizes the symmetrical transition state to a much greater extent than the ground state, in which the *tert*-butyl groups are wedged between the Cp rings. The net result is a high barrier to rotation in **8**. In the case of **1**, the bulkier PMe₃ ancillary ligand destabilizes the ground state geometry to a greater extent than in **8**, leading to a longer Ta-Si bond. However, the adverse silyl-PMe₃ interaction does not change much during rotation of the Ta-Si bond, whereas the long Ta-Si bond leads to a decrease in the Cp-silyl contacts in the transition state compared with **8**; thus the rotational barrier is lower for **1**. Additional thermodynamic consequences of the hindered rotation about the Ta-Si bonds in these bulky silyl complexes are discussed in section V.

IV. Mechanism of Activation of Arene C-H Bonds by 1. The inhibition by added PMe₃ of C-H activation by **1** strongly suggests that ligand dissociation is a necessary first step and that the 16e species Cp₂TaSi(*t*-Bu)₂H is a key intermediate. However, the question remains how this 16e intermediate interacts with C-H bonds. Several mechanisms have been established for C-H bond activation by various transition or f-block metal complexes. The most common mechanisms are oxidative addition of C-H bonds to unsaturated electron rich metal centers ("nucleophilic C-H activation"), typically found for electron rich late transition metal complexes,^{2,23} and four-center σ -bond metathesis pathways ("electrophilic C-H activation"), more commonly observed in electron deficient complexes of early transition or f-block metals.²⁴ In addition, a third general mechanism for C-H activation involving

metal-based radicals has been recently established by Wayland and co-workers.²⁵ In the present reaction, the nucleophilic pathway appears most likely because the silyl intermediate, Cp₂Ta(Si(*t*-Bu)₂H), contains a d² metal center, whereas the four-center mechanism is rarely observed for other than highly electrophilic d⁰ metal centers. More importantly, true oxidative addition to Ta(III) tantalocene complexes to yield Ta(V) species is well precedented, and the expected intermediate, Cp₂Ta(Ph)(H)(Si(*t*-Bu)₂H), is analogous to Cp₂Ta(CH₃)(H)(SiR₃) observed during the reaction of Cp₂Ta(CH₃)(PMe₃) with HSiR₃.¹⁷ This mechanism is similar to that originally proposed by Barefield, Parshall, and Tebbe for the Cp₂Ta(H)₃-catalyzed H/D exchange between H₂ and benzene-*d*₆, although in that instance the aryl intermediate was not observed.²⁶ The major difference is that in the present reaction the benzene C-H bond must add to the metal center in such a way that H, and not phenyl, lies in the central position next to the silyl ligands. Reductive elimination of silane and coordination of PMe₃ affords the observed products.

Additional evidence for an oxidative addition mechanism for C-H activation is found in the kinetic isotope effect (KIE), measured from the reaction of **1** with an equimolar mixture of benzene and benzene-*d*₆ at 25 °C. The ratio of **3/3-d**₅ was determined by ¹H NMR to be 1.7 ± 0.1:1 (average of three runs). Because the reverse reaction is extremely slow under these conditions, the ratio represents the kinetic preference for C-H activation, k_H/k_D . A KIE of 1.7 is consistent with a rate limiting transition state involving a bent Ta-H-C geometry, in which only a partial C-H bond breaking has occurred. The result also suggests that precoordination of benzene to form an η^2 -C₆H₆ complex is not occurring in the rate limiting step. In that case, only a small secondary isotope effect would be expected, as demonstrated by Jones and Feher for the reaction of "Cp*Rh(PMe₃)" with benzene ($k_H/k_D = 1.05$).^{23a} In comparison, a k_H/k_D value of 1.40 is reported for the actual C-H cleavage step. A very similar k_H/k_D value of 1.38 was reported by Janowicz and Bergman for the reaction of "Cp*Ir(PMe₃)" with cyclohexane.^{23b} In contrast, C-H activations by highly electrophilic systems via four-center mechanisms typically display much

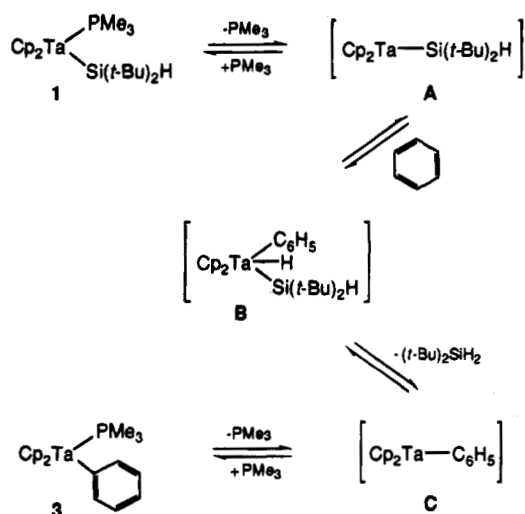
(23) See, for example: (a) Jones, W. D.; Feher, F. J. *J. Am. Chem. Soc.* **1986**, *108*, 4814. (b) Janowicz, A. H.; Bergman, R. G. *J. Am. Chem. Soc.* **1982**, *104*, 352. (c) Maguire, J. A.; Boes, W. T.; Goldman, M. E.; Goldman, A. S. *Coord. Chem. Rev.* **1990**, *97*, 179.

(24) (a) Thompson, M. E.; Baxter, S. M.; Bulls, A. R.; Burger, B. J.; Nolan, M. C.; Santasiero, B. D.; Schaefer, W. P.; Bercaw, J. E. *J. Am. Chem. Soc.* **1987**, *109*, 203. (b) Fendrick, C. M.; Marks, T. J. *J. Am. Chem. Soc.* **1986**, *108*, 425. (c) Watson, P. L. *J. Am. Chem. Soc.* **1983**, *105*, 6491. (d) Cummins, C. C.; Baxter, S. M.; Wolczanski, P. T. *J. Am. Chem. Soc.* **1988**, *110*, 8731. (e) Bruno, J. W.; Marks, T. J.; Day, V. W. *J. Am. Chem. Soc.* **1982**, *104*, 7357. (f) Fendrick, C. M.; Marks, T. J. *J. Am. Chem. Soc.* **1984**, *106*, 2214.

(25) (a) Wayland, B. B.; Ba, S.; Sherry, A. E. *J. Am. Chem. Soc.* **1991**, *113*, 5305. (b) Sherry, A. E.; Wayland, B. B. *J. Am. Chem. Soc.* **1990**, *112*, 1259.

(26) Barefield, E. K.; Parshall, G. W.; Tebbe, F. N. *J. Am. Chem. Soc.* **1970**, *92*, 5234.

Scheme 1



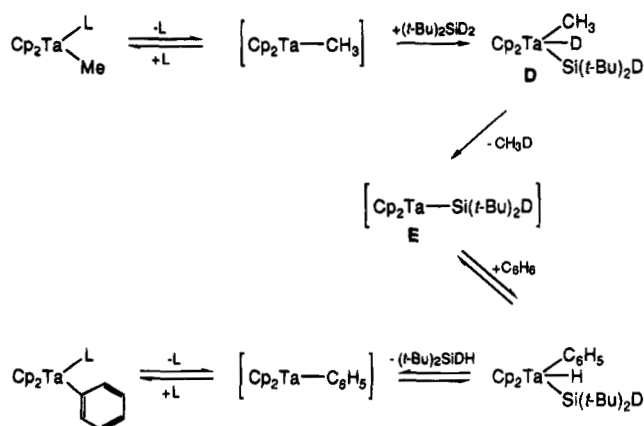
larger $k_{\text{H}}/k_{\text{D}}$ values in the range 3–6.^{24c-f} Metallo-radical activation of C–H bonds also appears to be characterized by large $k_{\text{H}}/k_{\text{D}}$ values.²⁵ Furthermore, radical pathways would be likely to show a preference for benzylic over aryl C–H activation, unlike the reactions of **1** with toluene and xylenes (vide supra).

A complete reaction sequence summarizing the factors discussed above is shown in Scheme 1. Generation of intermediate **A** by PMe_3 dissociation is believed to be the initial step. The arene C–H bond then adds to the metal center to give the 18e species **B**. Subsequent reductive elimination of silane followed by coordination of PMe_3 leads to the observed products. All of the steps are reversible, as demonstrated by the observation of mixtures of **1**, **3**, $\text{H}_2\text{Si}(\text{t-Bu})_2$, and benzene at equilibrium in cyclohexane solution. Quantitative analysis of this equilibrium is discussed in section V.

As described above, the different tantalum(III) complexes exhibit a remarkable difference in reactivity toward benzene C–H bonds. In particular, the alkyl and phenyl complexes are completely unreactive, whereas the silyls readily activate arenes. Assuming the mechanism depicted in Scheme 1 is operative, the origin of the difference would appear to be the failure of the 16e intermediates $\text{Cp}_2\text{Ta}(\text{R})$ ($\text{R} = \text{alkyl, aryl}$) to undergo C–H bond oxidative addition. The most likely cause of this difference is that silicon is much less electronegative than carbon ($\chi_{\text{C}} = 2.55$; $\chi_{\text{Si}} = 1.90$), leading to higher electron density at the metal in the silyl complexes, and hence a greater driving force for formation of the Ta(V) intermediates, $\text{Cp}_2\text{Ta}(\text{X})(\text{H})(\text{Ph})$. In other words, the silyl ligand is extremely electron releasing relative to hydrocarbyl ligands, which destabilizes the lower oxidation state at tantalum. Consistent with this premise, it is observed that “ Cp_2TaH ” ($\chi_{\text{H}} = 2.20$) also reacts with benzene, although the resulting Ta(V) species is not stable with respect to loss of benzene.²⁶

Support for the electron releasing nature of silyl ligands is also found in recent ab initio (MO/MP4) calculations by Sakaki and Ieki on bis(phosphine)-platinum complexes of silyl and alkyl ligands.²⁷ It was calculated that whereas the platinum–alkyl bond is polarized in the expected manner, $\text{Pt}^{\delta+}-\text{C}^{\delta-}$, silicon is sufficiently electron releasing for the silyl to be polarized

Scheme 2



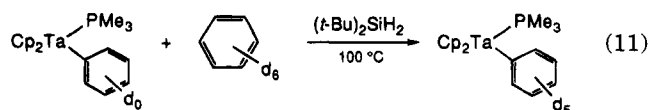
$\text{Pt}^{\delta-}-\text{Si}^{\delta+}$. Furthermore, the silicon in a platinum silyl carries a greater positive charge than even the parent hydrosilane, $\text{H}-\text{SiR}_3$, which leads to the interesting situation where H–Si “oxidative addition” to platinum results in partial oxidation of the silane and not the metal. Koga and Morokuma have also recently reported ab initio studies of metal–silicon compounds and attribute the strength of rhodium–silicon bonds to the strong σ -donating ability of the silyl ligand.²⁸

A variety of other transition metal silyl complexes also show unexpectedly high reactivity toward arene C–H bonds. For example, Tanaka and co-workers recently reported the platinum-catalyzed coupling of aryl C–H with *o*-bis(dimethylsilyl)benzene, in which a bis(silyl)-platinum species appears to be the active complex.^{14e} Furthermore, Ishikawa and co-workers have reported similar observations of catalytic C–H activation in a closely related nickel system.^{14f,g} In a related earlier report, Curtis observed formation of phenylsilanes in the redistribution of alkoxy silanes catalyzed by iridium silyl complexes and showed that the benzene solvent was the ultimate source of the aryl groups.²⁹ In all three cases the cleavage of arene C–H bonds appears to be more facile at metal centers with silyl ligands than with non-silyl analogs. Again, the enhanced reactivity of the low valent metal centers can be at least partially attributed to the strongly electron donating nature of silyl ligands.

The catalytic role of silanes in the reaction of **2** with benzene can be easily interpreted by the modified mechanism shown in Scheme 2. The 16e intermediate, $\text{Cp}_2\text{Ta}(\text{Me})$, is generated either thermally or photochemically and subsequently adds silane to form an 18e, Ta(V) species (**D**), which then reductively eliminates methane to yield the same Ta(III) silyl intermediate (**E**) which activates C–H bonds in Scheme 1. This proposal is supported by deuterium labeling experiments. When $(\text{t-Bu})_2\text{SiD}_2$ is used in the reaction of **2** with benzene, CH_3D is formed and hydrogen is incorporated into the silane. The reversibility of benzene oxidative addition and reductive elimination is confirmed by the silane-catalyzed phenyl ligand exchange between **3** and benzene- d_6 (eq 11). As described in section I, the phenyl ligand in compound **3** does not exchange with benzene- d_6 solvent at 100 °C in the absence of silane (eq 7). In the presence of di-*tert*-butylsilane, however, 80% ex-

(28) Koga, N.; Morokuma, K. *J. Am. Chem. Soc.* **1993**, *115*, 6883.

(29) Gustavson, W. A.; Epstein, P. S.; Curtis, M. D. *Organometallics* **1982**, *1*, 884.



change of the phenyl ligand is achieved within 4 h at the same temperature. The assumed irreversibility of methane reductive elimination has not been conclusively established, although **1** does not react with neat saturated hydrocarbons such as pentane and cyclohexane.

V. Thermodynamic Aspects of C–H Activation by $\text{Cp}_2\text{Ta}(\text{PMe}_3)(\text{SiR}_3)$. The observation of equilibrium mixtures in the reactions of the silyl complexes with benzene permits a more quantitative examination of the relative thermodynamics of C–H bond activation in these systems. Specifically, the temperature dependence of the equilibria allows ΔH° and ΔS° values to be calculated, and this enthalpy value can be used to estimate the relative strength of the Ta–Si bonds. Sealed tubes containing benzene and **1** (C_6D_{12} as solvent) or **6** (benzene- d_6 as solvent and reactant) were monitored by ^1H NMR at four temperatures (**1** 40, 50, 60, and 70 °C; **6** 90, 100, 110, and 120 °C) until equilibrium was achieved. The time required to reach equilibrium varied from almost 2 months at 40 °C to 10 days at 70 °C in the case of **1**, to 6 h at 90 °C and 2 h at 120 °C for the reaction of **6** with benzene. The concentrations of all species in solution were determined from peak areas obtained while the NMR probe was heated to the appropriate temperature, and equilibrium constants were calculated according to eq 12 (Tables 5 and 6). Van't Hoff plots of these data are shown in Figures 4 and 5, and corresponding values for the enthalpy and entropy of reaction are listed in Table 7.

$$K_{\text{eq}} = \frac{[\text{Cp}_2\text{Ta}(\text{PMe}_3)(\text{C}_6\text{H}_5)][\text{HSiR}_3]}{[\text{Cp}_2\text{Ta}(\text{PMe}_3)(\text{SiR}_3)][\text{C}_6\text{H}_6]} \quad (12)$$

The equilibrium constants for the reaction of **1** with benzene are fairly close to unity (0.7–3.1), whereas the measured values for the SiMe_3 complex are ca. 10^6 times smaller. Note that the measurement of two such disparate equilibrium constants by NMR was only possible by using very different initial concentrations of benzene and silane for the two cases. The large difference in K_{eq} is certainly consistent with the qualitative picture described in Section I, in which the bulky di-*tert*-butylsilyl complex reacts with benzene to a greater extent than **6**. Although it is tempting to view this steric destabilization of **1** as leading to a reduction of the bond dissociation enthalpy (BDE) of a specific bond such as the Ta–Si linkage, analysis of the data in Table 7 reveals this is a relatively small part of the story. In the case of the reaction of **6** with benzene (eq 4), the reaction is endothermic ($\Delta H^\circ = +12.3 \pm 0.6$ kcal mol $^{-1}$), and the modest favorable entropy change (7 ± 2 eu) only provides ca. 2–3 kcal mol $^{-1}$ of driving force in the temperature range studied. Therefore, ΔG for the reaction is dominated by the unfavorable enthalpy change. A small value for ΔS° is reasonable for eq 4, as there is no net change in the number of molecules during the reaction.

The reaction of **1** with benzene (eq 1) is also endothermic ($\Delta H^\circ = +10.8 \pm 0.6$ kcal mol $^{-1}$), but as expected, the enthalpy change is less unfavorable than for eq 4 ($\Delta\Delta H^\circ = 1.5$ kcal mol $^{-1}$). This is far short of

Table 5. Equilibrium Constants (K_{eq}) and ΔG for the Reaction of **1 with Benzene**

temp (K)	K_{eq}	ΔG (kcal mol $^{-1}$)
313	0.68 ± 0.02	0.24 ± 0.1
323	1.15 ± 0.02	-0.09 ± 0.1
333	1.96 ± 0.02	-0.44 ± 0.1
343	3.05 ± 0.02	-0.76 ± 0.1

Table 6. Equilibrium Constants (K_{eq}) and ΔG for the Reaction of **6 with Benzene**

temp (K)	$10^6 K_{\text{eq}}$	ΔG (kcal mol $^{-1}$)
363	1.5 ± 0.1	9.7 ± 0.1
373	2.4 ± 0.1	9.6 ± 0.1
383	3.7 ± 0.1	9.5 ± 0.1
393	5.5 ± 0.1	9.4 ± 0.1

Table 7. Thermodynamic Parameters for Reactions **1, **4**, and **13**^b**

reaction	K_{eq}^a (at 298 K)	ΔG° (kcal mol $^{-1}$)	ΔH° (kcal mol $^{-1}$)	ΔS° (eu)
1 + C_6H_6 (eq 1)	0.32	0.7 ± 0.1	10.8 ± 0.6	34 ± 3
6 + C_6D_6 (eq 4)	3.3×10^{-8}	10.2 ± 0.1	12.3 ± 0.6	7 ± 2
1 + Me_3SiH (eq 13) ^b	1.1×10^7	-9.6	-1.6	27

^a Extrapolated to 298 K. ^b Calculated using values from the first two rows.

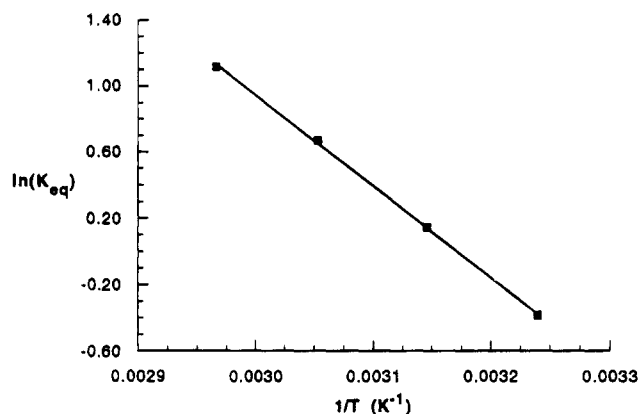


Figure 4. Van't Hoff plot for the reaction of **1** with benzene.

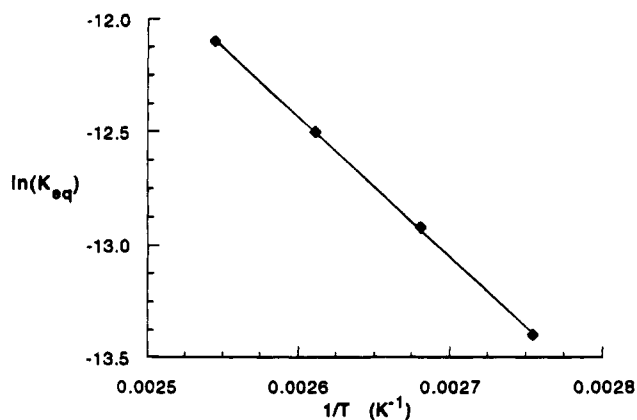


Figure 5. Van't Hoff plot for the reaction of **6** with benzene.

the amount needed to explain the large difference in K_{eq} observed. However, the entropy change for eq 1 is quite large and favorable (34 ± 3 eu). In this instance the $T\Delta S^\circ$ term is comparable to ΔH° in the temperature range examined; thus the net free energy change is nearly zero. Indeed, the data in Table 5 show that ΔG for eq 1 changes sign between 313 and 323 K. It is

calculated that at 318 K the enthalpy and entropy contributions exactly cancel and $\Delta G = 0$ ($K_{\text{eq}} = 1$).

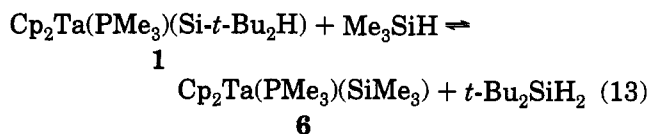
The apparent conclusion from the above analysis is rather surprising: The relative thermodynamic instability of the sterically encumbered silyl complex **1** does not arise principally from the enthalpic term, which would be typically associated with strained and weakened bonds, but rather from a favorable entropy change which is not significant in the case of the less hindered silyl **6**. Given that the molecularity of eq 1 is the same as for eq 4 (i.e., two particles in equilibrium with two particles), the large discrepancy in ΔS° for the two reactions is not immediately obvious, and the origin of this effect deserves further consideration. Clearly, it is the large ΔS° for eq 1 (34 eu) that is anomalous at first glance. The extrapolation to infinite temperature required by any Van't Hoff type plot can introduce significant error in the calculated ΔS° value; however, the discrepancy between eqs 1 and 4 is reproducible and is much less than the likely error in the individual values. The temperature dependence of the equilibrium constants was determined by two totally independent series of experiments, both of which yielded statistically identical results: (eq 1, 33 and 35 eu;³⁰ eq 4, both 7 eu).

Another possible source of the large entropy gain in eq 1 is differential solvation of starting materials and products. This can be broken down into two aspects, the size of the solute's cavity in the solvent and the nature of the solute-solvent interactions.³¹ It should be borne in mind in the following discussion that all the tantalum complexes involved in eqs 1 and 4 are 18e, saturated species; therefore solvent-solute interactions will be outer-sphere in nature. It has been shown that there is a relationship between the size of the cavity caused by a solute in a solvent and the resulting entropy of solvation. For example, in one instance it was observed that a change in solvation entropy from -23.6 to -13.3 eu resulted from decreasing the molecular radii by a factor of 2.³² Although -Si(H)(*t*-Bu)₂ is a large ligand, the overall radius of Cp₂Ta(PMe₃)(SiH(*t*-Bu)₂) is only 7-10% larger than that of the SiMe₃ or phenyl derivatives. It is therefore unlikely that such a small size difference will give rise to such a substantial artifact in the entropy analysis as observed here.

Another potential concern regarding the entropy of eq 1 is that the equilibria 1 and 4 had to be measured in different solvents, C₆D₆ and C₆D₁₂. However, it has been shown that the secondary sphere organizations (i.e., nonspecific coordination) of benzene and cyclohexane around solutes are virtually identical, leading to comparable values of ΔG , ΔH , and ΔS of solvation.^{32b,33} It is unlikely, therefore, that this factor could be the sole source of the large deviation of ΔS° for eq 1. Because there is no change in the number of particles during the reaction of **1** or **6** with benzene, it would appear then that the entropy change must be due to changes in internal degrees of freedom in going from the reactants to products. The task is then to determine whether 34 eu is anywhere near a reasonable value for

the standard entropy of reaction 1, when some or all degrees of freedom are absent or hindered in one or both sides of the reaction.

Although precise calculation of the standard entropies of molecules as large and complicated as these tantalum complexes is not feasible, useful approximate values can be derived using Benson's approach, which assumes the additivity of thermodynamic parameters within related systems.³⁴ Because group entropy values have not been tabulated for Ta-Si or Ta-C bonds, calculation of S° for **1** or **6**, and hence estimation of ΔS° for eq 1 or 4, is not possible. However, this obstacle can be surmounted by considering the silyl exchange reaction shown in eq 13, in which **1** reacts with HSiMe₃ to yield **6** and H₂Si(*t*-Bu)₂.



Unfortunately, eq 13 is too exergonic for K_{eq} to be directly measured using the NMR methods employed for eqs 1 and 4. However, both eqs 1 and 4 employ benzene as a reactant and generate the phenyl complex **2** as the product; therefore, subtraction of eq 4 from eq 1 yields eq 13. Furthermore, Hess law allows the derivation of the thermodynamic parameters for eq 13 by subtracting those for eq 4 from eq 1 (Table 7). Thus ΔS° for eq 13 is 27 eu, nearly as large as for eq 1, which still reflects the anomalous entropy contribution of the bulky complex **1**. Benson's analysis of the entropy of reaction 13, assuming free rotation of all bonds in reactants^{35a} and products,^{35b} yields a calculated ΔS° of only 1.4 eu, as expected for an equilibrium involving no change in the number of particles. However, as described in sections II and III, the combination of the Cp₂Ta coordination environment with the bulky Si(*t*-Bu)₂H group in **1** leads to severe steric crowding, manifested in an extremely long Ta-Si bond and solution dynamics that are comparable to the NMR time scale. A comparable Benson-type analysis, assuming completely hindered rotation of all rotors in **1**, yields a calculated ΔS° of +34.0 eu³⁶ or somewhat larger than the value of 27 eu calculated from the equilibrium measurements. Of course, it is obvious that the molecular rotors in **1** do not actually stop, but rather face higher rotational barriers in **1** than in **6**; thus the observed value of ΔS° should be less than that estimated above. The symmetry number corrections used in these calculations correspond to a classical limit in statistical mechanics.³⁴ Precise analysis of this situation involves a quantum mechanical treatment and knowledge of the rotational partition functions for each rotor. Furthermore, it is likely that the internal rotations in **1** are more highly correlated with one another than in **6**, and thus have fewer degrees of freedom even when "freely" rotating.³⁷ Although a more sophisticated analysis of the problem

(30) A preliminary third independent determination, which was carried out at 35, 45, 55, and 65 °C and where equilibria have almost been established, gave $\Delta S^\circ = 29$ eu.

(31) Abraham, M. H.; Grellier, P. L. *Can. J. Chem.* **1988**, *66*, 2673.

(32) (a) Abraham, M. H. *J. Am. Chem. Soc.* **1979**, *101*, 5477. (b) Abraham, M. H.; Nasehzadeh, A. *J. Chem. Soc., Faraday Trans.* **1981**, *77*, 321.

(33) Abraham, M. H. *J. Am. Chem. Soc.* **1981**, *103*, 6742.

(34) Benson, S. W. *Thermochemical Kinetics*, 2nd ed.; Wiley: New York, 1976.

(35) (a) HSiMe₃: $R \ln(3 \times 3^3/1) = 8.7$ eu. The ground state of **1** is chiral (see Experimental Section) and thus its correction is given by $R \ln(1 \times 5^2 \times 3^3 \times 3 \times 3^6 \times 3^2/2) = 31.2$ eu. (b) 18.8 eu for H₂Si(*t*-Bu)₂ ($=R \ln(2 \times 3^6 \times 3^2/1)$) and 22.5 eu for **6** ($=R \ln(1 \times 5^2 \times 3^3 \times 3 \times 3^3 \times 3/2)$). The ground state of **6** is also chiral.¹⁷

(36) $\Delta S^\circ = 41.3 - (-R \ln(2) + 8.7)$ eu.

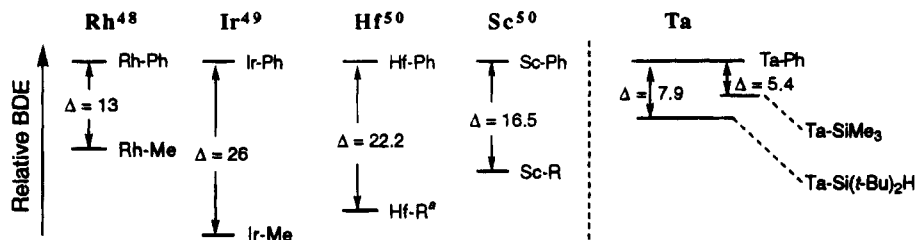


Figure 6. Metal-alkyl and -silicon BDE's relative to the phenyl analogs. The relative positions of M-Ph bonds have been arbitrarily set equal, and no absolute correlation between the columns is implied. Δ values are in units of kcal mol⁻¹. (*R = CH₂CH₂CH₂C₆Me₄.)

is well outside the scope or interests of the present report, the approximate treatment does give some confidence that relief of steric congestion in the bulky silyl **1** could provide an entropy change of the magnitude observed for eq 1 and calculated for eq 13.

VI. Relative Tantalum-Silicon and Tantalum-Carbon Bond Strengths. It was established in the preceding section that the major difference in the energetics of C-H activation by **1** and **6** is in the magnitude of the entropy change. However, the standard enthalpy changes determined for eqs 1 and 4 also provide information and can be used to estimate the strength of Ta-Si bonds relative to the Ta-C bond of the phenyl complex **3**. If the principal of functional group thermochemical additivity holds,³⁴ ΔH° for reactions 1 and 4 will be equal to the sum of the BDE's of the Ta-Si and Ph-H bonds broken minus the BDE's of the Ta-Ph and Si-H bonds formed.^{5a,38} This equation can be rearranged to solve for the difference between the Ta-Si and Ta-Ph BDE (eq 14).

$$[D(\text{Ta-Si}) - D(\text{Ta-C})] = \Delta H^\circ - [D(\text{C-H}) - D(\text{Si-H})] \quad (14)$$

The BDE of a C-H in benzene is 110.9 kcal mol⁻¹,³⁹ and the value for the Si-H in Me₃Si-H is ca. 93.2 kcal mol⁻¹.⁴⁰⁻⁴⁴ Combining these BDE's with the enthalpy change of 12.3 kcal mol⁻¹ for eq 4 yields a difference of -5.4 kcal mol⁻¹. In other words, the Ta-SiMe₃ bond in **6** is weaker than the Ta-phenyl bond in **3** by 5.4 kcal mol⁻¹.⁴⁵ Furthermore, using an approximate value of 92.2 kcal mol⁻¹ for the Si-H BDE in di-*tert*-butylsilane,⁴⁶ it is calculated that the hindered Ta-Si bond in **1** is weaker than the Ta-Ph bond in **3** by 7.9 kcal mol⁻¹.

Unfortunately, since there have been no calorimetric determinations of Ta-Si or Ta-Ph BDE's, it is not possible to place the BDE's determined in the present study on an absolute scale. The *average* Ta-C BDE in TaMe₅ was determined by reaction solution calorimetry to be 62.4 kcal mol⁻¹,⁴⁷ but the steric and electronic environments in this compound are too different from those of the Cp₂Ta(PMe₃)(R) derivatives for the Ta-Me BDE to be of any quantitative value. However, the strength of the Ta-Si bond relative to the Ta-Ph bond is in itself informative. Recent studies have shown that metal-phenyl bonds are stronger than the corresponding metal-alkyl bonds by ca. 5-20 kcal mol⁻¹, depending on the specific system.⁴⁸⁻⁵⁰ This mirrors the trend

in C-H BDE's: Bonds to sp² carbons are stronger than those to sp³ centers. Relative BDE's of alkyl and phenyl complexes are shown graphically in Figure 6, in which the M-Ph BDE's are arbitrarily set equal. The relative Ta-Si BDE's determined in this study are shown to the right in Figure 6. Unfortunately, the difference between Ta-Ph and Ta-Me BDE's has not been measured, but it is reasonable to assume it will be similar to the M-alkyl/M-phenyl BDE differences in the representative complexes shown in Figure 6. This leads to the conclusion that the Ta-Si BDE is comparable to and probably greater than that of the Ta-alkyl bond. This idea gains further support in light of the absolute U-Si BDE recently determined by solution calorimetry. Marks and co-workers found that the U-Si BDE in Cp⁺₃U-SiPh₃ (Cp⁺ ≡ η⁵-C₅H₄SiMe₃) is 37.3 ± 4.0 kcal mol⁻¹.¹⁵ Although the triphenyl substitution would be expected to lead to a particularly low U-Si BDE on the basis of

(37) On the basis of the variable temperature ¹H NMR and crystal structures of **1** and **6**, the best analogy is with rapidly rotating, intermeshed gears. Decoalescence of Cp or SiMe₃ resonances was not observed in the case of **6** even at 193 K.

(38) The validity of employing BDE's measured in the gas phase in this type of calculation is persuasively argued in ref 5a.

(39) McMillen, D. F.; Golden, D. M. *Annu. Rev. Phys. Chem.* **1982**, *33*, 493.

(40) The BDE's for Me₃Si-H, and for silanes in general, have been extensively debated. Common reference books⁴¹ continue to grossly underestimate the values by as much as 25 kcal mol⁻¹, but the extensive studies of Walsh^{42,43} and others⁴⁴ indicate that Si-H BDE's for alkylsilanes fall in a narrow range of ca. 89-95 kcal mol⁻¹. Recent studies indicate that Walsh's original value for the Si-H BDE in Me₃SiH should be revised upward from 90.8 to ca. 93.2 kcal mol⁻¹ (390 kJ mol⁻¹), with error limits of ca. ±2 kcal mol⁻¹.^{43,44a}

(41) (a) Gordon, A. G.; Ford, R. A. *The Chemists Companion*; Wiley: New York, 1972. (b) Lowry, T. H.; Richardson, K. S. *Mechanism and Theory in Organic Chemistry*; Harper and Row: New York, 1981.

(42) For excellent reviews, see: (a) Walsh, R. *Acc. Chem. Res.* **1981**, *14*, 246. (b) Walsh, R. In *The Chemistry of Organic Silicon Compounds*; Patai, S., Rappoport, Z., Eds.; Wiley: New York, 1989; Vol. 2, Chapter 5.

(43) (a) Pilcher, G.; Leitão, M. L. P.; Meng-Yan, Y.; Walsh, R. *J. Chem. Soc., Faraday Trans.* **1991**, *87*, 841. (b) R. Walsh, private communication.

(44) (a) Marshall, P.; Ding, L. *J. Am. Chem. Soc.* **1992**, *114*, 5754. (b) Wetzel, D. M.; Salomon, K. E.; Berger, S.; Brauman, J. I. *J. Am. Chem. Soc.* **1989**, *111*, 3835.

(45) Because eq 4 was measured in C₆D₆, the exchange involved Ph-D and Si-D bonds. Both of these R-D bonds are slightly stronger than the R-H analog, due to the lower zero point energy on the R-D potential energy surface. However, the Δ BDE's for Ph-D/Ph-H and Si-D/Si-H will be nearly equal, and ignoring this factor introduces at most an error of ca. 0.5 kcal mol⁻¹ into the calculation of the relative Ta-Si BDE.

(46) The Si-H BDE in H₂Si(*t*-Bu)₂ has not been measured but will be within 1-2 kcal mol⁻¹ of that in Me₃SiH₂. The latter value was originally reported as 89.3 kcal mol⁻¹,⁴² but should be revised upward to 92.2 kcal mol⁻¹ as described above.^{40,43,44a}

(47) Adedji, F. A.; Connor, J. A.; Skinner, H. A.; Galyer, L.; Wilkinson, G. J. *J. Chem. Soc. Chem. Commun.* **1976**, 159.

(48) Jones, W. D.; Feher, F. J. *J. Am. Chem. Soc.* **1984**, *106*, 1650.

(49) Stoutland, P. D.; Bergman, R. G.; Nolan, S. P.; Hoff, C. D. *Polyhedron* **1988**, *7*, 1429.

(50) Bulls, A. R.; Bercaw, J. E.; Manriques, J. M.; Thompson, M. E. *Polyhedron* **1988**, *7*, 1409.

both steric and electronic considerations, this value is comparable to the U-C BDE's in $\text{Cp}^+_3\text{U}-(n\text{-Bu})$ ($28.9 \pm 1.7 \text{ kcal mol}^{-1}$), $\text{Cp}^+_3\text{U}-\text{CH}_2\text{SiMe}_3$ ($39.3 \pm 2.3 \text{ kcal mol}^{-1}$), and $\text{Cp}^+_3\text{U}-\text{Me}$ ($44.8 \pm 1.1 \text{ kcal mol}^{-1}$).⁵¹ Unfortunately, the strength of the U-Si bond relative to the uranium-phenyl bond cannot be ascertained, as the value for $\text{Cp}^+_3\text{U}-\text{Ph}$ was not reported. It is likely, however, that the U-Ph BDE is equal to or greater than that in the vinyl derivative, $\text{Cp}^+_3\text{U}-\text{CH}=\text{CH}_2$ ($48.5 \pm 2.2 \text{ kcal mol}^{-1}$).⁵¹ This would make the U-Si bond weaker by at least 10 kcal mol^{-1} and thus comparable to the 5-8 kcal mol^{-1} found for the tantalocene silyl/phenyl system. Furthermore, relative to the metal alkyl BDE, the metal silyl BDE would be expected to be greater for a tantalum(III) complex such as **1** and **6** than in an electrophilic f-element complex.²⁸

The thermochemistry of metal silyl compounds has also been explored by ab initio calculations, as reported by two groups recently.^{27,28} Both studies indicate that late metal-silicon bonds are ca. 20 kcal mol^{-1} stronger than the corresponding alkyl bonds. Interestingly, both reports also suggest the origin of the strong metal-silicon bonds is the σ -donor strength of the silyl, not π -back-bonding from the metal to silicon. Koga and Morokuma²⁸ also examined the strength of Zr-C and Zr-Si bonds and found that the order is reversed; i.e., the metal alkyl BDE in the d^0 , early metal, complex is greater than the metal silyl BDE. This observation was interpreted as being due to the poorer σ -acceptor ability of the electropositive metal, which does not interact as strongly with the σ -donating silyl ligand. Another interesting aspect of the ab initio result is the prediction that, other factors being equal, metal silicon BDE's will decrease going from late to early transition metals, whereas metal carbon BDE's increase, reflecting in both cases the difference in electronegativities between the metal and the ligand. It is well-known that partial ionic character leads to stronger covalent bonds,⁵² and the relative strength of late metal silicon bonds can be interpreted in this light. Furthermore, the bonds between silicon and the Ta(III) center in the present studies should be intermediate in polarity between the Zr(IV)-silicon and the late metal-silicon bonds considered in the theoretical treatments. The observation that the Ta-Si BDE's are comparable to or slightly stronger than Ta-alkyl BDE's is thus consistent with the theoretical prediction.

Conclusions

In summary, tantalum silyl complexes, $\text{Cp}_2\text{Ta}(\text{PMe}_3)(\text{SiR}_3)$, activate the C-H bonds of unhindered arenes such as benzene, toluene, and *m*-xylene to yield equilibrium mixtures containing the tantalum aryl complex and corresponding hydrosilane. Only in the case of neat arene solutions of the extremely hindered di-*tert*-butyl-silyl complex, $\text{Cp}_2\text{Ta}(\text{PMe}_3)(\text{Si}(t\text{-Bu})_2\text{H})$, does the reaction proceed completely to the aryl complexes. Although smaller silyls are reactive toward these C-H bonds, in this instance the silyl complexes are thermodynamically favored over the aryls. The mechanism of the C-H bond activation appears to be a simple oxidative addi-

tion of the C-H bond to a 16e intermediate, " $\text{Cp}_2\text{Ta}(\text{SiR}_3)$ ", generated by phosphine dissociation.

Although the steric bulk of the $\text{Si}(t\text{-Bu})_2\text{H}$ ligand does lead to a slightly weaker Ta-Si bond than in the Ta-SiMe₃ derivative, a major source of destabilization of the more sterically congested complex **1** is the loss of entropy due to partially hindered internal rotations. Thus the differences in reactivity of **1** and **6** are largely entropic in origin, not enthalpic. This is an excellent example of the risks associated with the common assumption that only bond strengths need to be considered in predicting the driving force for reactions.

The Ta-Si BDE's in $\text{Cp}_2\text{Ta}(\text{PMe}_3)(\text{SiR}_3)$ are found to be only ca. 5-8 kcal mol^{-1} weaker than the Ta-Ph bond in $\text{Cp}_2\text{Ta}(\text{PMe}_3)(\text{Ph})$ and are probably comparable to or greater than the corresponding Ta-alkyl BDE's. This fact, together with the greater strength of C-H BDE's compared with Si-H BDE's, makes the reaction of metal-hydrocarbyl complexes with hydrosilanes extremely energetically favorable for most metal complexes.^{15-17,53}

Experimental Section

General Procedures. All reactions and manipulations were carried out using either high vacuum line techniques or a glovebox under an atmosphere of prepurified N₂. Solvents were distilled from sodium benzophenone ketyl before use. All photolyses were carried out in a Rayonet photochemical reactor with low pressure mercury arc lamps (350 nm). ¹H NMR spectra were recorded on an IBM AC-250 NMR spectrometer. The temperature inside the NMR probe was calibrated by measuring the temperature dependence of the chemical shift difference between the hydroxyl protons and the hydrogens on the carbons of ethylene glycol ($T > 273 \text{ K}$) and methanol ($T < 273 \text{ K}$) samples.^{41a} ¹³C NMR spectra were obtained at 125.76 MHz on a Bruker AM-500 spectrometer equipped with a ¹H/¹³C dual probe. ³¹P NMR spectra were obtained at 81.02 MHz on a Bruker AF-200 spectrometer equipped with a broadband multinuclear probe. Benzene-*d*₆ was used as the NMR solvent unless otherwise indicated. The ¹H and ¹³C NMR spectra are referenced to SiMe₄, and ³¹P NMR spectra are referenced to external standard 85% H₃PO₄. Elemental analyses were performed by Robertson Microlit, Inc. Infrared measurements were made on a Perkin-Elmer 1430 spectrophotometer and calibrated against polystyrene films. High resolution mass spectra were obtained on a VG Instrument ZAB-E spectrometer using chemical ionization by Mr. John Dykins at the University of Pennsylvania. $\text{Cp}_2\text{Ta}(\text{PMe}_3)(\text{Si}(t\text{-Bu})_2\text{H})$,¹⁷ $\text{Cp}_2\text{Ta}(\text{PMe}_3)(\text{Si}(t\text{-Bu})_2\text{H})$,¹⁷ $\text{Cp}_2\text{Ta}(\text{PMe}_3)(\text{SiMe}_3)$,¹⁷ $\text{Cp}_2\text{Ta}(\text{CO})(\text{SiMe}_3)$,¹⁷ $\text{Cp}_2\text{Ta}(\text{CH}_2=\text{CH}_2)(\text{CH}_3)$,⁵⁴ $\text{Cp}_2\text{Ta}(\text{PMe}_3)(\text{CH}_3)$,⁵⁴ and $\text{Cp}_2\text{Ta}(\text{PMe}_3)(\text{SiMe}_2\text{H})$ ⁵⁵ were prepared as previously described. (*t*-Bu)₂SiH₂ (gift from Lithco) was dried over molecular sieves and degassed before use.

Preparation of $\text{Cp}_2\text{Ta}(\text{PMe}_3)(\text{Ph})$ (3**).** (a) From $\text{Cp}_2\text{Ta}(\text{PMe}_3)(\text{Me})$, **2**. A solution of **2** (500 mg, 1.24 mmol) and H₂-Si(*t*-Bu)₂ (206 mg, 1.43 mmol) in 10 mL of benzene was heated at 100 °C for 4 h. The mixture was then filtered and volatiles were removed in vacuum to yield 528 mg of dark red **3** (92%). Although **3** appeared pure by NMR, satisfactory elemental analyses could not be obtained, despite repeated recrystallization. Repeated submissions for analysis yielded carbon percentages which were unreproducibly low. Similar problems were encountered with the other phenyl derivatives, **5** and **11**. NMR: Table 1. HRMS: *m/e* calcd for C₁₉H₂₄PTa: 464.110. Found: 464.105. Anal. Calc for C₁₉H₂₄PTa: C, 49.15; H, 5.21. Found: C, 51.13; H, 5.36.

(51) Schock, L. E.; Seyam, A. M.; Sabat, M.; Marks, T. J. *Polyhedron* **1988**, *7*, 1517.

(52) Pauling, L. *The Nature of the Chemical Bond*, 3rd ed.; Cornell University Press: Ithaca, NY, 1960.

(53) Thorn, D. L.; Harlow, R. L. *Inorg. Chem.* **1990**, *29*, 2017.

(54) Schrock, R. R.; Hoffmann, R. *J. Am. Chem. Soc.* **1978**, *100*, 2389.

(55) Berry, D. H.; Jiang, Q. *J. Am. Chem. Soc.* **1987**, *109*, 6211.

(b) From $\text{Cp}_2\text{Ta}(\text{PMe}_3)(\text{Si}(t\text{-Bu})_2\text{H})$, **1**. A solution of **1** (50 mg, 0.09 mmol) in 15 mL of benzene was heated at 70 °C for 3 h. Removal of all volatiles, followed by recrystallization from *n*-pentane, gave 39 mg of **3** (89%).

Preparation of $\text{Cp}_2\text{Ta}(\text{PMe}_3)(m\text{-Xyl})$ (5**).** A solution of **2** (140 mg, 0.348 mmol) and $\text{H}_2\text{Si}(t\text{-Bu})_2$ (70 mg, 0.485 mmol) in 18 mL of xylene was heated at 85 °C for 6 h. All volatiles were then removed and the product was recrystallized from toluene/petroleum ether to yield 140 mg of purple **5** (82%). NMR: Table 1. HRMS: *m/e* calcd for $\text{C}_{21}\text{H}_{28}\text{PTa}$: 492.141. Found: 492.143. Anal. Calc for $\text{C}_{21}\text{H}_{28}\text{PTa}$: C, 51.23; H, 5.73. Found: C, 47.01; H, 4.97. See comment above regarding the analysis of aryl complexes.

Preparation of $\text{Cp}_2\text{Ta}(\text{CH}_2=\text{CH}_2)(\text{Ph})$ (11**).** A solution of $\text{Cp}_2\text{Ta}(\text{CH}_2=\text{CH}_2)(\text{CH}_3)$ (200 mg, 0.56 mmol) and $\text{H}_2\text{Si}(t\text{-Bu})_2$ (100 μL , 0.63 mmol) in 10 mL of benzene was irradiated (low pressure mercury lamps, 350 nm) at 40–50 °C for 6 h. The solution was filtered, and all volatiles were removed in vacuum. The residue was recrystallized from toluene/hexanes to yield 80 mg of **11**. A second crop of 45 mg was collected from the sublimation of the nonvolatile residue of the mother liquor. Total yield: 125 mg, 55%. NMR: Table 1. HRMS: *m/e* calcd for $\text{C}_{18}\text{H}_{19}\text{Ta}$: 416.10. This parent ion was not detected; rather the fragment corresponding to the loss of ethylene was observed. Calculated for $\text{C}_{16}\text{H}_{15}\text{Ta}$: 388.065. Found: 388.064. Anal. Calc for $\text{C}_{18}\text{H}_{19}\text{Ta}$: C, 51.93; H, 4.60. Found: C, 47.47; H, 4.14. See comment above regarding the analysis of aryl complexes.

Reaction of $\text{Cp}_2\text{Ta}(\text{PMe}_3)(\text{Si}(t\text{-Bu})_2\text{H})$ (1**) with Benzene.** A sealed NMR tube containing **1** (10 mg, 0.019 mmol) and benzene (20 μL , 0.21 mmol) in 0.5 mL of cyclohexane-*d*₁₂ was heated at 65–70 °C and monitored by ¹H NMR. Complete conversion to **3** and $\text{H}_2\text{Si}(t\text{-Bu})_2$ was achieved in 2.5 h.

Reaction of $\text{Cp}_2\text{Ta}(\text{PMe}_3)(\text{Si}(t\text{-Bu})_2\text{H})$ (1**) with Benzene-*d*₆.** A sealed NMR tube containing **1** (10 mg, 0.019 mmol) and 0.5 mL of benzene-*d*₆ was heated at 65–75 °C and monitored by ¹H NMR. Complete conversion of **3-d**₅ and (D)(H)Si(*t*-Bu)₂ was achieved within 2 h.

Reaction of $\text{Cp}_2\text{Ta}(\text{PMe}_3)(\text{Si}(t\text{-Bu})_2\text{H})$ (1**) with Toluene.** A solution of **1** (10 mg, 0.019 mmol) in 1 mL of toluene was heated at 80 °C for 3 h. Volatiles were removed under vacuum, and the nonvolatile residue was dissolved in 0.5 mL of benzene-*d*₆. ¹H NMR showed complete conversion to the tolyl complex $\text{Cp}_2\text{Ta}(\text{PMe}_3)(\text{C}_7\text{H}_7)$ (**4a,b**; mp = 2:1). No *o*-tolyl or benzyl complexes were observed by ¹H NMR. ¹H, ¹³C, and ³¹P NMR chemical shifts are listed in Table 1.

Reaction of $\text{Cp}_2\text{Ta}(\text{PMe}_3)(\text{Si}(t\text{-Bu})_2\text{H})$ (1**) with *m*-Xylene.** A solution of **1** (10 mg, 0.019 mmol) in 1 mL of *m*-xylene was heated at 80 °C for 3 h. Volatiles were removed under vacuum, and the nonvolatile residue was dissolved in 0.5 mL of benzene-*d*₆. ¹H NMR showed complete conversion to the *m*-xylyl complex $\text{Cp}_2\text{Ta}(\text{PMe}_3)(m\text{-Xyl})$ (**5**). No other isomers were identified by ¹H NMR.

Attempted Reaction of $\text{Cp}_2\text{Ta}(\text{PMe}_3)(\text{Si}(t\text{-Bu})_2\text{H})$ (1**) with *p*-Xylene.** A solution of **1** (10 mg, 0.019 mmol) in 1 mL of *p*-xylene was heated at 65–75 °C for 2.5 h. Volatiles were removed in vacuum, and the nonvolatile residue was dissolved in 0.5 mL of benzene-*d*₆. ¹H NMR showed ca. 70% of **1** remained unreacted, while 30% was converted to several unidentified products.

Attempted Reaction of $\text{Cp}_2\text{Ta}(\text{PMe}_3)(\text{Si}(t\text{-Bu})_2\text{H})$ (1**) with Mesitylene.** A solution of **1** (10 mg, 0.019 mmol) in 1 mL of mesitylene was heated at 80 °C for 3 h. Volatiles were removed in vacuum, and the nonvolatile residue was dissolved in 0.5 mL of benzene-*d*₆. ¹H NMR showed that ca. 80% of **1** remained unreacted and 20% was converted to several unidentified compounds.

Reaction of $\text{Cp}_2\text{Ta}(\text{PMe}_3)(\text{SiMe}_3)$ (6**) with Benzene.** A sealed NMR tube containing $\text{Cp}_2\text{Ta}(\text{PMe}_3)(\text{SiMe}_3)$ (**6**) (10 mg, 0.022 mmol) in 0.5 mL of benzene-*d*₆ was heated at 100 °C for 2 h. The ¹H NMR of the sample showed that small amounts (ca. 2%) of **3-d**₅ and DSiMe₃ were formed.

Reaction of $\text{Cp}_2\text{Ta}(\text{PMe}_3)(\text{SiMe}_2\text{H})$ (7**) with Benzene.** A sealed NMR tube containing $\text{Cp}_2\text{Ta}(\text{PMe}_3)(\text{SiMe}_2\text{H})$ (**7**) (10 mg, 0.022 mmol) and 0.5 mL of benzene-*d*₆ was heated at 100 °C for 6 h. The ¹H NMR of the sample showed that the Si–H signal at δ 4.85 was partially deuterated (~40%). However, no $\text{Cp}_2\text{Ta}(\text{PMe}_3)(\text{Ph})$ (**3**) was formed.

Reaction of $\text{Cp}_2\text{Ta}(\text{PMe}_3)(\text{CH}_3)$ (2**) with Benzene.** A sealed NMR tube containing **2** (5 mg, 0.013 mmol) and 0.5 mL of benzene-*d*₆ was heated at 100 °C and monitored by ¹H NMR. After 1.5 h, ca. 10% starting material decomposed with only trace amounts of **3-d**₅ formed (ca. 1% of total tantalum compounds). After 25 h, ca. 50% of **2** decomposed with only 3% (of all tantalum compounds) of **3-d**₅ formed. A small amount of CH₄ (not CH₃D) was also observed.

Reaction of **1 with Benzene in the Presence of Added PMe_3 .** A solution of **1** (20 mg, 0.037 mmol) in 1 mL of benzene-*d*₆ was divided into two NMR tubes. To one tube was added PMe_3 (0.055 mmol), and the tubes were sealed. After 3 days at 25 °C, ¹H NMR spectra of the samples showed 50% conversion to **3-d**₅ in the tube without PMe_3 and only 12% conversion in the tube with PMe_3 present.

Reaction of $\text{Cp}_2\text{Ta}(\text{PMe}_3)(\text{CH}_3)$ (2**) with Benzene in the Presence of $\text{H}_2\text{Si}(t\text{-Bu})_2$.** A sealed NMR tube containing **2** (6 mg, 0.015 mmol) and $\text{H}_2\text{Si}(t\text{-Bu})_2$ (5 μL , 0.031 mmol) in 0.5 mL of benzene-*d*₆ was heated at 100 °C and monitored by ¹H NMR. 90% conversion to **3-d**₅ and CH₄ was achieved within 1.5 h.

Deuteration of $\text{Cp}_2\text{Ta}(\text{PMe}_3)(\text{C}_6\text{H}_5)$ (3**) with C_6D_6 in the Presence of $\text{H}_2\text{Si}(t\text{-Bu})_2$.** A solution of **3-d**₀ (10 mg, 0.022 mmol) in 1 mL of benzene-*d*₆ was divided into two NMR tubes. To one tube was added $\text{H}_2\text{Si}(t\text{-Bu})_2$ (3 μL , 0.019 mmol), and the tubes were sealed. Reactions in these two tubes were monitored by ¹H NMR. After 4 h at 100 °C, the sample with silane present showed 80% deuteration (by integration) of the phenyl group. The sample without silane showed no deuteration and prolonged heating (16 h) resulted in decomposition. A third NMR tube containing 15 mg of $\text{Cp}_2\text{Ta}(\text{PMe}_3)(\text{C}_6\text{H}_5)$ (0.019 mmol) and 8 μL of $\text{H}_2\text{Si}(t\text{-Bu})_2$ (0.050 mmol) in benzene-*d*₆ (0.5 mL) was kept in the dark at 25 °C for 11 days. The ¹H NMR of this sample showed the formation of only trace amounts of C_6H_6 , but no observable deuteration of the phenyl group.

Reaction of $\text{Cp}_2\text{Ta}(\text{PMe}_3)(\text{CH}_3)$ (2**) with Benzene in the Presence of HSiMe_3 .** A sealed NMR tube containing **2** (10 mg, 0.025 mmol) and HSiMe_3 (0.006 mmol) in 0.5 mL of benzene-*d*₆ was heated at 100 °C for 2 h. The ¹H NMR spectrum of the sample showed that 70% of **2** had converted to two major products: **3** (45%) and **6** (25%). The formation of CH₄ was also detected.

Kinetic Isotope Effect for the Reaction of **1 with Benzene.** A solution of **1** (30 mg, 0.057 mmol) in 1.61 mL of a 1:1 mixture of benzene and benzene-*d*₆ (0.80 mL of benzene-*d*₆, 0.81 mL of benzene) was divided into three ampoules. The ampoules were sealed off and submerged in a 25.0 °C water bath. A NMR tube containing 10 mg of $\text{Cp}_2\text{Ta}(\text{PMe}_3)(\text{Si}(t\text{-Bu})_2\text{H})$ in benzene-*d*₆ was kept under the same conditions to monitor the reactions in the ampoules. After 3 days at 30 °C, the ¹H NMR spectrum of the NMR sample showed complete conversion to $\text{Cp}_2\text{Ta}(\text{PMe}_3)(\text{Ph})$. All volatiles in the ampoules were removed under vacuum, and the residue in each ampoule was dissolved in cyclohexane-*d*₁₂ and transferred to an NMR tube. *k_H/k_D* ratios were determined by careful integration of the Cp and C_6H_5 resonances in the ¹H NMR spectra of the three samples collected with long relaxation times. The average value of *k_H/k_D* thus obtained was 1.7 ± 0.1.

Thermodynamic Measurements. Reaction of **1 with Benzene (eq 1).** Two independent determinations of the equilibrium constants at each temperature were carried out, each measured as follows. A solution of **1** (42 mg, 0.079 mmol), benzene (12 μL , 0.134 mmol), $\text{H}_2\text{Si}(t\text{-Bu})_2$ (8 μL , 0.050 mmol), and hexamethylbenzene (8.6 mg, 0.053 mmol, internal standard) in 2.0 mL of cyclohexane-*d*₁₂ was divided into four NMR

tubes, and the tubes were sealed. The tubes were heated at 40, 50, 60, and 70 °C, respectively, until equilibrium in each tube was reached (monitored by ^1H NMR). The concentration of each component was determined by integration of resonances in the ^1H NMR spectrum relative to the internal standard, obtained while the probe was heated to the corresponding temperature.

Reaction of 6 with Benzene (Eq 4). Two independent determinations of the equilibrium constants at each temperature were carried out, each measurement done as follows. A solution of **6** (33 mg, 0.088 mmol) and hexamethylbenzene (5.6 mg, 0.035 mmol, internal standard) in benzene- d_6 (1.626 g, 19.36 mmol) was divided into four NMR tubes, and the tubes were sealed. The tubes were heated at 90, 100, 110, and 120 °C, respectively, until equilibrium in each tube was reached (monitored by ^1H NMR). The concentration of benzene- d_6 was calculated from the density of the pure liquid (0.95 g cm^{-3}) as 11.29 M. The concentration of other components were measured by integration referenced to the internal standard in the ^1H NMR spectrum obtained while the probe was heated to the corresponding temperature.

Structure Determinations of 1, 8, and 9. Single crystals of suitable size were grown from toluene/hexanes at $-35\text{ }^\circ\text{C}$ and sealed in 0.5-mm thin-walled Pyrex capillaries in the glovebox. The capillaries were then mounted on the diffractometer. Refined cell dimensions and their standard deviations were obtained from least squares refinements of 25 accurately centered reflections with $2\theta > 25^\circ$. Crystal data are summarized in Table 2.

Diffraction data were collected at 295 K on an Enraf-Nonius CAD-4 diffractometer employing graphite-monochromated Mo $K\alpha$ radiation ($\lambda = 0.71073\text{ \AA}$) and using the ω - 2θ scan technique. Three standard reflections measured every 3500 s of X-ray exposure showed no intensity decay over the course of the data collections. Data collection is summarized in Table 2. The raw intensities were corrected for Lorentz and polarization effects by using the program BEGIN from the SDP+ package.⁵⁶ Empirical absorption corrections based on ψ scans were applied as indicated.

All calculations were performed on a DEC Mircovax 3100

computer with the SPD+ software package.⁵⁶ The structures were solved by standard heavy atom Patterson techniques followed by weighed Fourier syntheses. The full-matrix least squares refinements were based on F , and the function minimized was $\sum w(|F_o| - |F_c|)^2$ with $w = 1/\sigma^2(F)$. Atomic scattering factors and complex anomalous dispersion corrections were taken from refs 57 and 58. Non-hydrogen atoms were refined anisotropically and hydrogen atoms were included as constant contributions to the structure factors and were not refined. Agreement factors are defined as $R_1 = \sum||F_o| - |F_c||/\sum|F_o|$ and $R_2 = [\sum w||F_o| - |F_c||^2/\sum w|F_o|^2]^{1/2}$. The goodness of fit is defined as $\text{GOF} = [\sum w(|F_o| - |F_c|)^2/(N_o - N_p)]^{1/2}$, where N_o and N_p are the numbers of observations and parameters.

Choice of the acentric space group $P2_1P2_1P2_1$ (No. 19) for complexes **1** and **9** was confirmed by examination of several Bijvoet reflections which did not average satisfactorily following absorption correction. Correct enantiomorph assignment in each case was confirmed by refinement of the other enantiomorph to significantly higher agreement factors.

Acknowledgment. Financial support of this work by the Petroleum Research Fund and the National Science Foundation is gratefully acknowledged. We also thank Terry Rathman of Lithco for a generous gift of $(t\text{-Bu})_2\text{SiH}_2$.

Supplementary Material Available: Tables of positional parameters, anisotropic thermal parameters, and bond distances and angles for **1**, **8**, and **9** (20 pages). Ordering information is given on any current masthead page.

OM940328Z

(56) B. A. Frenz and Associates, Inc., College Station, TX 77840, and Enraf-Nonius, Delft, Holland.

(57) *International Tables for X-Ray Crystallography*; Kynoch: Birmingham, England, 1974; Vol. IV, Tables 2.2B and 2.3.1.

(58) Sewart, R. F.; Davidson, E. R.; Simpson, W. T. *J. Chem. Phys.* **1965**, *42*, 3175–3187.